AN ABSTRACT OF THE THESIS OF

Evon P. Silvia for the degree of Master of Science in Civil Engineering presented on June 1, 2011.

Title: Overcoming the Level Bubble: Terrestrial Laser Scanning Reference Frame Transformations

Abstract approved:

_____

Michael J. Olsen

Terrestrial Laser Scanning (TLS) is an efficient, effective, and precise measurement tool rapidly growing in popularity in a wide variety of fields. Use of TLS data often requires aligning multiple scans for a more complete model of a scene or object, a procedure known as scan registration. Each scan setup must be transformed (*i.e.*, rotated, scaled, and translated) and adjusted to match the other setups as closely as possible. This research investigates and compares the traditional least squares method against a rapid, noniterative technique recently proposed and develops possible solutions to achieve the strengths of both methods.

Additionally, modern TLS instruments are commonly equipped with an inclination sensor to measure deviations from a level setup in order to simplify the registration process. This thesis investigates the reliability, usefulness, and

limitations of these sensors. In particular, the concept of a “stability threshold” that ensures reliable inclination measurements in modern, rapid scanners is introduced and sources of inclination sensor error, and procedures to minimize that error, are investigated. While level and unlevel setups appear to produce consistent results, full 360° scan windows measured in both the clockwise and counter-clockwise direction are recommended.

Finally, some field applications of TLS reference frame transformations are presented and discussed, including the development of a coordinate system in a large-scale research laboratory and steps toward the development of real-time change detection.

Overcoming the Level Bubble: Terrestrial Laser Scanning Reference Frame Transformations

by
Evon P. Silvia

A THESIS

submitted to

Oregon State University

in partial fulfillment of
the requirements for the
degree of

Master of Science

Presented June 1, 2011
Commencement June 2011

Master of Science thesis of Evon P. Silvia presented on June 1, 2011.

APPROVED:

_____

Major Professor, representing Civil Engineering

_____

Head of the School of Civil and Construction Engineering

_____

Dean of the Graduate School

I understand that my thesis will become part of the permanent collection of Oregon State University libraries. My signature below authorizes release of my thesis to any reader upon request.

_____

Evon P. Silvia, Author

ACKNOWLEDGEMENTS

I would like to thank my committee members Michael Wing, Mike Bailey, and especially Robert Schultz for their patience and time, and for their assistance reviewing this thesis. I could not have started working toward my Masters without the support of the immortal Prof. Schultz.

Dr. Mike Olsen deserves my sincerest appreciation for taking me on as a grad student within half an hour of our first meeting, for expediting the paperwork to get me into grad school, for persevering whenever I got difficult, and for always finding enough funding to keep me going. Your patience, understanding, flexibility, and instruction made the grad school experience rewarding, even if I didn't pursue a PhD like you wanted!

Thanks to Amber Clark and Dr. Tom Dick for your thought-provoking help with the mathematics.

Finally, a big thanks goes to my brother and sisters who stayed up late with me while I worked on my papers, homework, and projects and who tolerated me when I got inevitably sleep-deprived and loopy.

CONTRIBUTION OF AUTHORS

Dr. Michael Olsen assisted with the interpretation of the mathematics and data in Chapter 2. He also contributed to the experimental design, editing, analysis, and direction of Chapter 3.

Tim Maddux provided the historical data and access to the O. H. Hinsdale Wave Research Laboratory presented in Chapters 3 and 4.

Shawn Butcher assisted with data collection.

TABLE OF CONTENTS

TABLE OF CONTENTS (Continued)

Page

TABLE OF CONTENTS (Continued)

LIST OF FIGURES

LIST OF FIGURES (Continued)

LIST OF FIGURES (Continued)

Figure | Page

LIST OF TABLES

LIST OF APPENDIX FIGURES

This document is dedicated to my Lord and Savior, Jesus Christ, who brought me through a tumultuous fall term and without whom I would have no reason to leave my home in the first place.

1 INTRODUCTION

Humans have attempted to measure the earth for millennia, a task that continues to grow in complexity and precision to this day. Land surveyors are professionals in this field, seeking to locate objects in a two- or three-dimensional reference frame. Advancements in computers, microprocessors, and the ability to measure—and define—time at very fine resolutions have had a direct impact on the tools of the surveying profession, revolutionizing the industry over the past two decades, just as it has impacted our everyday lives (Anderson and Mikhail 1998).

Recently, laser scanning, or Light Detection And Ranging (LiDAR), has emerged as a very reliable, efficient, and accurate measurement technique with successful implementation in a wide variety of applications including, for example, CAD model verification (*e.g.*, Son, Park and Lee 2002; Ravani, et al. 2007), historic site and feature preservation (*e.g.*, Bernardini, et al. 2002), crime scene reconstruction (*e.g.*, Agosto, et al. 2008), topographic surveying (*e.g.*, Wehr and Lohr 1999), forest resource management (*e.g.*, Wynne 2006), landslide modeling (*e.g.*, Dunning, Rosser and Massey 2010), and coastal erosion studies (*e.g.*, Olsen, et al. 2009).

1.1 LASER SCANNING OVERVIEW

For a detailed overview of laser scanning the reader is referred to Vosselman and Maas (2010). Only a basic overview is presented herein. The modern

laser scanner is an active sensor that emits a beam of light (a laser pulse) toward a remote object, measures the time-of-flight to and from the object, and computes the distance between the remote object and the scanner. While the intricacies of measuring the time-of-flight vary by system, the distance from the scanner to the object (the “range”) is calculated using the following equation:

$$L = 0.5 c_a \Delta t \tag{1.1}$$

where L is the distance from the scanner to the object, c_a is the speed of light under the current atmospheric conditions (299,792,458 m/s in a vacuum), and Δt is the time-of-flight of the laser pulse. Scanner measurement frequencies are typically on the order of tens of thousands of pulses per second (JADA Productions 2010), conducted while simultaneously rotating the scanner mirror along a given range of horizontal (ϕ) and vertical (ψ) angles (Figure 1). Some newer scanners can conduct full waveform analysis, enabling the recording of multiple returns per pulse. The set of 3D points collected from one or more scans is referred to as a “point cloud.”

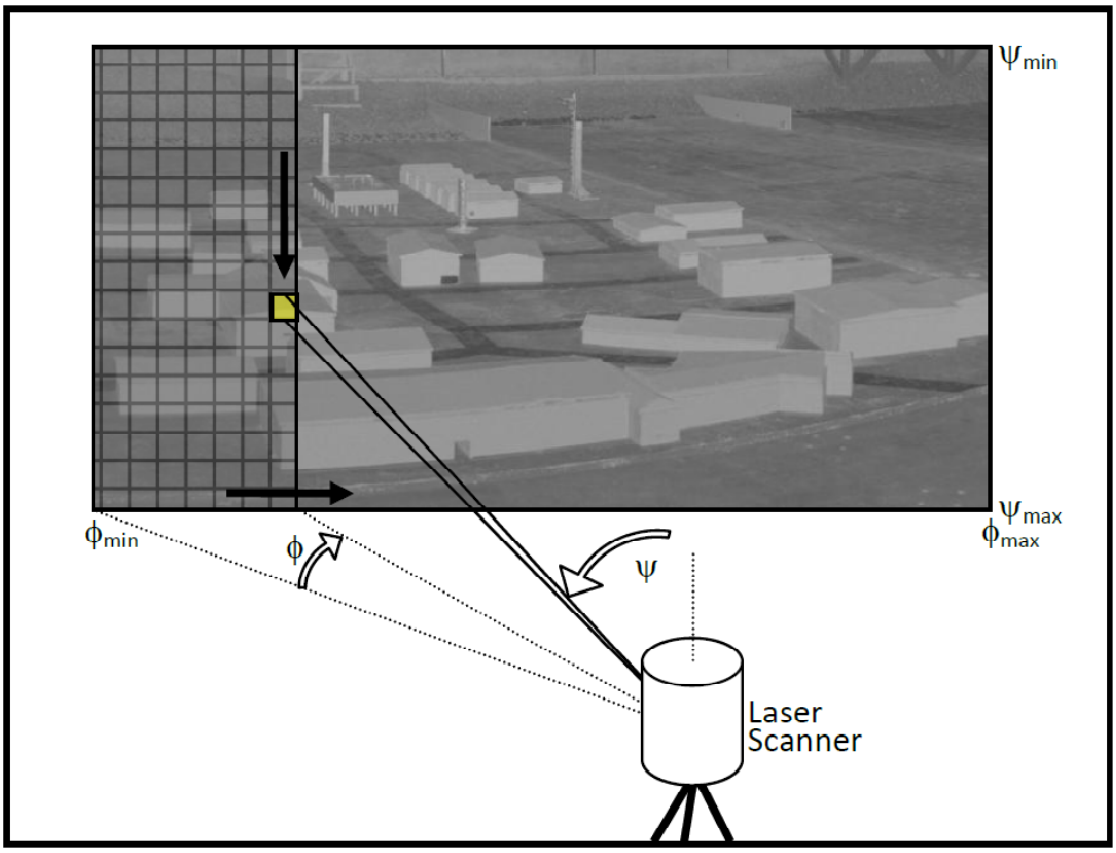

Figure 1: Scanners rotate horizontally (ϕ) and vertically (ψ), recording thousands of points per second.

All laser scanners are also line-of-sight instruments, meaning that they can only measure the visible surfaces of objects as seen from the setup location. Therefore multiple scans are usually required for full coverage of an area or object. Figure 2 demonstrates the use of two additional scan setups to fill gaps (black regions) present in the original scan (left) due to occlusions.

Because each setup, or scan position, has its own spherical coordinate system based on the location and orientation of the scanner, each scan must

be shifted and rotated to be aligned to a common reference frame. This process is known generally as scan registration, or georeferencing if a geographic coordinate system is used. Multiple options have been developed to register scans together, although most implement some form of a least squares adjustment to minimize the difference between common targets at known locations (target registration), common points (cloud-to-cloud registration), or common objects (surface registration). For more detail see Section 3.2.1 of the thesis and Vosselman and Maas (2010).

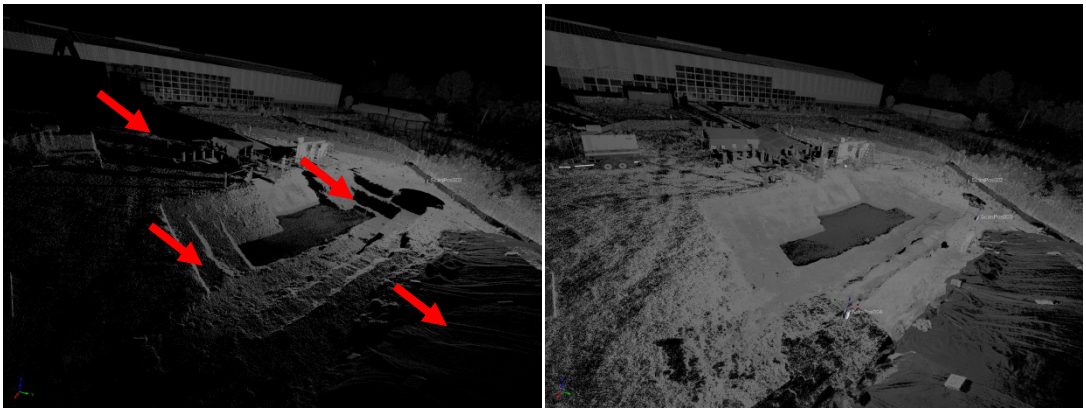

Figure 2: Laser scanners are line-of-sight instruments, resulting in occlusions. This soil pit was scanned from one (left) and three (right) scan positions, filling occlusions (red arrows) using multiple scan positions.

Laser scanners generally have three different implementations, each with its own advantages. The simplest mode is terrestrial laser scanning (TLS), which entails mounting the instrument on a static setup such as a tripod, where it remains for the duration of the scan. Mobile scanning extends this concept

with GPS and an IMU (Inertial Measurement Unit) by mounting the scanner on an automobile or boat for rapidly modeling a corridor such as a highway or river without interrupting the flow of traffic or exposing field crew to vehicle traffic (Barber, Mills and Smith-Voysey 2008). Finally, airborne laser scanning ("ALS" among geomatics professionals or simply "LiDAR" in other contexts) takes mobile scanning into the air on a plane or helicopter for terrain or forest modeling (Wehr and Lohr 1999). Point clouds produced by these methods are usually processed in the office, although research to interact with the data in real time is ongoing (Skaloud, et al. 2010).

1.2 THESIS FORMAT

This document follows the manuscript thesis format.

Chapter 2 introduces the basic principles of transforming point data between reference frames. The adjustment of TLS-related point data will also be discussed, covering both traditional least squares adjustment methods and a noniterative approach developed by Han (2010b). The shortcomings and effectiveness of each method will be discussed.

Chapter 3 presents a technical manuscript currently under review for publication in the ASCE Journal of Surveying Engineering on applications and assessments of inclination sensors in terrestrial laser scanning. The

manuscript also includes a case study demonstrating the value of inclination sensors for discovering control network errors.

Chapter 4 extends the discussion of the new O. H. Hinsdale Wave Research Laboratory control coordinate system introduced in Chapter 3 to summarize considerations that arose in its development. Also presented will be an application of TLS reference frame transformations for real-time change detection, including a custom interface developed to expand the capabilities of the scanner used in this research.

Chapter 5 summarizes the conclusions and contributions of this thesis and presents further study made possible by this research. The appendices contain user manuals for the tools developed to accomplish this research.

Note that throughout this document the terms “coordinate system” and “reference frame” will be used interchangeably.

2 TRANSFORMATION AND ADJUSTMENT OF POINT DATA

The location of a single point in three-dimensional space can be described using a Cartesian (*X, Y, Z*) coordinate system. Conceptually, for example, the Rose Garden in Portland, Oregon can be described as being a certain distance east (*X*), north (*Y*), and above (*Z*) the Portland State University campus. That same point also has another set of Cartesian coordinates measured relative to downtown Portland, and yet another set relative to the peak of Mount Hood. The point's physical location in space never actually changes, but the *X*, *Y*, and *Z* values of its coordinates will be dramatically different in each coordinate system, or reference frame. The process of converting point coordinates from one reference frame to another is known as transformation.

Please note that throughout this section, all coordinate systems and rotations will strictly follow the right-hand rule (see Figure 3). Equations, notation, and order of operations vary between sources, but the theory remains generally the same. Least squares equations and transformation equations have been adapted from Ghilani (2010) except where noted.

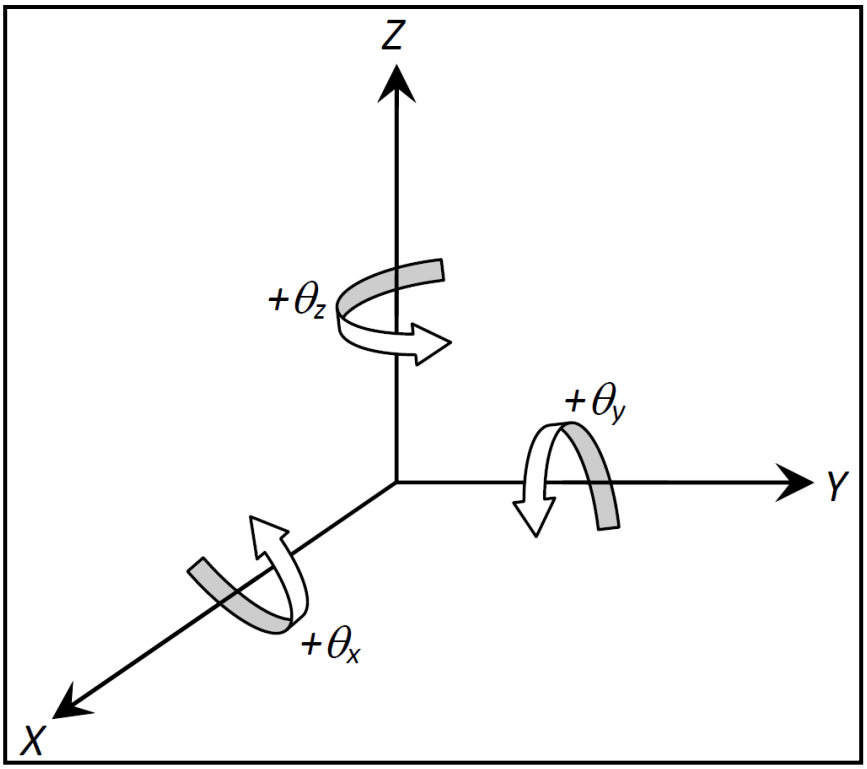

Figure 3: A right-handed coordinate system with positive rotations shown.

2.1 Transformation Between Reference Frames

Suppose a point, $\boldsymbol{P_0}$, in one reference frame is a vertical vector with coordinates *x*, *y*, and *z*. Or,

$$\boldsymbol{P_0} = \begin{bmatrix} x \\ y \\ z \end{bmatrix} \tag{2.1}$$

Converting a set of coordinates from one reference frame to another is known as *transformation*, broken down into a three-step process of rotation, scaling, and translation.

These transformations can also be described using a quaternion, which represents a single rotation about a vector (Jekeli 2001). A quaternion can be computationally efficient and avoids the singularity problem known as gimbal lock, and will be integrated into future research. The approaches analyzed in this section do not use quaternions.

2.1.1 Rotation

The rotation of a reference frame around its origin can be described as a rigid body rotation using three angles known as roll (θ_x), or rotation around the *X*-axis, pitch (θ_y), or rotation around the *Y*-axis, and yaw (θ_z), or rotation around the *Z*-axis. These angles are all measured relative to the original reference frame. The rotation of a point's coordinates into a new reference frame using any one of those angles can be accomplished by multiplying $\boldsymbol{P_0}$ by one of the following matrices:

$$\boldsymbol{R_x} = \begin{bmatrix} 1 & 0 & 0 \\ 0 & \cos\theta_{\mathrm{x}} & \sin\theta_{\mathrm{x}} \\ 0 & -\sin\theta_{\mathrm{x}} & \cos\theta_{\mathrm{x}} \end{bmatrix} \tag{2.2a}$$

$$\boldsymbol{R_y} = \begin{bmatrix} \cos\theta_{\mathrm{y}} & 0 & -\sin\theta_{\mathrm{y}} \\ 0 & 1 & 0 \\ \sin\theta_{\mathrm{y}} & 0 & \cos\theta_{\mathrm{y}} \end{bmatrix} \tag{2.2b}$$

$$\boldsymbol{R_z} = \begin{bmatrix} \cos\theta_{\mathrm{z}} & \sin\theta_{\mathrm{z}} & 0 \\ -\sin\theta_{\mathrm{z}} & \cos\theta_{\mathrm{z}} & 0 \\ 0 & 0 & 1 \end{bmatrix} \tag{2.2c}$$

The combined effect of $\boldsymbol{R_x}$, $\boldsymbol{R_y}$, and $\boldsymbol{R_z}$ can be summarized as

$$\boldsymbol{P_R} = \boldsymbol{R_z R_y R_x P_0} = \boldsymbol{R P}_0 \tag{2.3}$$

where $\boldsymbol{R}$ is the combined 3x3 transformation matrix of the three axial rotation matrices and $\boldsymbol{P_R}$ is the point vector in the rotated reference frame. Note that matrix multiplication is not commutative, so $\boldsymbol{R} = \boldsymbol{R_x R_y R_z}$ would result in a different rotation matrix. Multiplying the matrices together in order from left to right, such that r_{nm} is the element of $\boldsymbol{R}$ corresponding to row n and column m, produces

$$\boldsymbol{R} = \begin{bmatrix} r_{11} & r_{12} & r_{13} \\ r_{21} & r_{22} & r_{23} \\ r_{31} & r_{32} & r_{33} \end{bmatrix} \tag{2.4}$$

$$r_{11} = \cos\theta_{\mathrm{y}} \cos\theta_{\mathrm{z}}$$

$$r_{12} = \cos\theta_{\mathrm{x}} \sin\theta_{\mathrm{z}} + \sin\theta_{\mathrm{x}} \sin\theta_{\mathrm{y}} \cos\theta_{\mathrm{z}}$$

$$r_{13} = \sin\theta_{\mathrm{x}} \sin\theta_{\mathrm{z}} - \cos\theta_{\mathrm{x}} \sin\theta_{\mathrm{y}} \cos\theta_{\mathrm{z}}$$

$$r_{21} = -\cos\theta_{\mathrm{y}} \sin\theta_{\mathrm{z}}$$

$$r_{22} = \cos\theta_{\mathrm{x}} \cos\theta_{\mathrm{z}} - \sin\theta_{\mathrm{x}} \sin\theta_{\mathrm{y}} \sin\theta_{\mathrm{z}}$$

$$r_{23} = \sin\theta_{\mathrm{x}} \cos\theta_{\mathrm{z}} + \cos\theta_{\mathrm{x}} \sin\theta_{\mathrm{y}} \sin\theta_{\mathrm{z}}$$

$$r_{31} = \sin\theta_{\mathrm{y}}$$

$$r_{32} = -\sin\theta_{\mathrm{x}} \cos\theta_{\mathrm{y}}$$

$$r_{33} = \cos\theta_{\mathrm{x}} \cos\theta_{\mathrm{y}}$$

Roll, pitch, and yaw can be extracted from the rotation matrix in (2.4) by

$$\begin{bmatrix}\theta_x\\ \theta_y\\ \theta_z\end{bmatrix} = \begin{bmatrix}\arctan\left(\frac{-r_{32}}{r_{33}}\right)\\ \arctan\left(\frac{r_{31}}{\sqrt{r_{11}^2+r_{21}^2}}\right)\\ \arctan\left(\frac{-r_{21}}{r_{11}}\right)\end{bmatrix} \tag{2.5}$$

A rotation matrix is a special orthogonal matrix and as a result must demonstrate certain properties (Vuylsteker 2004):

1. The inverse of ***R*** is equal to the transpose ($\boldsymbol{R}^{-1} = \boldsymbol{R}^{T}$).
2. The determinant of ***R*** = +1.
3. The sum of the squares for any row or column in ***R*** equals 1.
4. The dot product of any pair of rows or any pair of columns in ***R*** is 0.
5. The rows of ***R*** represent the unit vector components in the original reference frame along the axes of the rotated reference frame.
6. The columns of ***R*** represent the unit vector components in the rotated reference frame along the axes of the original reference frame.

Property 3, the usefulness of which will be shown in Section 2.2.5, can be written explicitly as

$$r_{11}{}^2 + r_{12}{}^2 + r_{13}{}^2 = 1$$
$$r_{21}{}^2 + r_{22}{}^2 + r_{23}{}^2 = 1$$
$$r_{31}{}^2 + r_{32}{}^2 + r_{33}{}^2 = 1$$

$$r_{11}{}^2 + r_{21}{}^2 + r_{31}{}^2 = 1$$
$$r_{12}{}^2 + r_{22}{}^2 + r_{32}{}^2 = 1$$
$$r_{13}{}^2 + r_{23}{}^2 + r_{33}{}^2 = 1 \quad (2.6)$$

After rotation, $\boldsymbol{P_R}$ is then scaled and translated relative to the rotated reference frame to complete the transformation.

2.1.2 Scale

Scaling point coordinates can follow either a similarity model, with a uniform scale factor, or an affine model, where scale factors for each axis must be determined.

Scale factors in TLS are usually used to model atmospheric effects and can also be used to convert topographic measurements to grid distances with a grid scale factor. Atmospheric corrections to the range values for the instrument used in this study are modeled using the following guidelines and standard values (RIEGL LMS GmbH 2011):

- A change in temperature of +1 °C yields a change in correction of +1 ppm (calibrated at 12 °C).
- A change in air pressure of +10 millibars yields a change in correction of -2.7 ppm (calibrated at 1000 mbar).
- A change in relative humidity from 0% to 100% yields a change in correction of only 0.5 ppm (calibrated at 60%).

While the instrument used in this study automatically applies atmospheric corrections during measurement, this may not always be the case with other instruments.

Since grid scale factors and atmospheric corrections are generally assumed to be constant throughout the project site, a similarity model is usually sufficient for laser scanning applications. Affine models are more common in photogrammetry, where directional-dependent scale changes due to photograph distortion can occur (Han 2010b).

2.1.3 Translation

Rigid translation of $\boldsymbol{P_R}$ is accomplished by adding a translation vector, ***T'***, to the point, shifting it relative to the new origin. Note that ***T'*** is in the new reference frame; its components would be different in the original reference frame if translation is applied prior to rotation.

2.1.4 Transformation Summary

In matrix form, the full three-dimensional transformation of point $\boldsymbol{P_0}$ from one reference frame into another can be described with the following equation:

$$\boldsymbol{P'} = S\boldsymbol{R}\boldsymbol{P_0} + \boldsymbol{T'}$$

$$\begin{bmatrix} X' \\ Y' \\ Z' \end{bmatrix} = S \begin{bmatrix} r_{11} & r_{12} & r_{13} \\ r_{21} & r_{22} & r_{23} \\ r_{31} & r_{32} & r_{33} \end{bmatrix} \begin{bmatrix} x \\ y \\ z \end{bmatrix} + \begin{bmatrix} T_x' \\ T_y' \\ T_z' \end{bmatrix} \quad (2.7)$$

Thus, seven parameters are required for a three-dimensional similarity transformation: S, θ_x, θ_y, θ_z, T_x, T_y, and T_z.

2.2 POINT DATA ADJUSTMENT

Every measurement contains error (Lichti, Gordon and Tipdecho 2005). Thus even if a given set of points were measured twice under identical conditions using a single instrument in perfect condition, two slightly different sets of point data would be produced.

Assuming that only random error is present (*i.e.,* no mistakes or blunders were made and systematic error has been minimized or eliminated), any effort to match the two data sets together optimally would evenly distribute the error among the input parameters. By definition, least squares adjustment methods produce the most mathematically "correct" match between two data sets by minimizing the sum of the square of the errors (Ghilani 2010). A simple average is a special case of least squares that can be applied to measurements of a single quantity. The least squares approach requires equations to be linearized, and requires iterative solutions when applied to nonlinear equations such as the transformations discussed previously.

Han (2010b) developed a noniterative alternative to least squares methods using eigentheory known as the "noniterative solution to linear transformations," or NISLT (Han, Guo and Chou 2011).

Fundamentally, both methods attempt to compute the seven parameters for a three-dimensional similarity transformation introduced in Section 2.1 that would result in the closest match of one data set to another.

The following sections will introduce the basic concepts of both methods and compare their strengths and weaknesses. See also Ghilani (2010), Han (2010a), Han (2010b), and Han, Guo, and Chou (2011).

2.2.1 Least Squares Adjustment – General Case

Given a set of linear equations relating an equal number of independent unknowns ($x_1, x_2, \ldots, x_n$), a unique solution can be found. If redundant data with errors is collected, multiple solutions exist. A solution that minimizes the sum of the square of the errors can be computed:

$$\boldsymbol{A^T A X = A^T L} \tag{2.8a}$$

where $\boldsymbol{A}$ is a stacked matrix of the coefficients of the linear equations, $\boldsymbol{X}$ is a vertical vector of the unknowns, and $\boldsymbol{L}$ is a vertical vector containing the right-hand side of the linear equations. Solving for $\boldsymbol{X}$ will give the solution:

$$\boldsymbol{X = (A^T A)^{-1} A^T L} \tag{2.8b}$$

Weighting can also be introduced to each measurement using the diagonal matrix $\boldsymbol{W}$, often the inverse of the standard deviation of the measurements:

$$\boldsymbol{X} = (\boldsymbol{A^T W A})^{-1}\boldsymbol{A^T W L} \tag{2.8c}$$

However, if the equations are nonlinear, they must be linearized prior to implementation in the least squares solution, often using a first-order Taylor series approximation. Finding a solution becomes an iterative process that must begin with approximations of the final solution, ***X***, and each iteration computes corrections, ***e***, to be applied to the previous guess. In matrix form,

$$\boldsymbol{e} = (\boldsymbol{J^T W J})^{-1}\boldsymbol{J^T W K} \tag{2.9}$$

where

$$\boldsymbol{e} = \begin{bmatrix} dx_1 \\ dx_2 \\ \vdots \\ dx_n \end{bmatrix} \quad \boldsymbol{J} = \begin{bmatrix} \frac{\partial F_1}{\partial x_1} & \frac{\partial F_1}{\partial x_2} & \cdots & \frac{\partial F_1}{\partial x_n} \\ \frac{\partial F_2}{\partial x_1} & \frac{\partial F_2}{\partial x_2} & \cdots & \frac{\partial F_2}{\partial x_n} \\ \vdots & \vdots & \ddots & \vdots \\ \frac{\partial F_m}{\partial x_1} & \frac{\partial F_m}{\partial x_2} & \cdots & \frac{\partial F_m}{\partial x_n} \end{bmatrix} \quad \boldsymbol{K} = \begin{bmatrix} l_1 - F_1(x_1, x_2, \ldots, x_n) \\ l_2 - F_2(x_1, x_2, \ldots, x_n) \\ \vdots \\ l_m - F_m(x_1, x_2, \ldots, x_n) \end{bmatrix}$$

W is the weighting matrix as in (2.8c), F_1 through F_m is the set of original normal equations, ***J*** is a Jacobian Matrix of the partial derivatives of the normal equations, and l_1 through l_m are the elements from ***L*** in (2.8c). With each iteration, ***e*** is added to ***X*** and the process is repeated until the corrections in ***e*** are sufficiently small.

2.2.2 Least Squares Adjustment – Reference Frames

In the case of computing the seven parameters for a three-dimensional similarity transformation that minimizes the overall error, an iterative approach is required since (2.7) is nonlinear. Each point used in the computation contributes three equations; therefore, a unique solution requires, at minimum, three non-collinear points. Using a traditional least squares adjustment, four non-coplanar points are required to prevent gimbal lock (Jekeli 2001). Gimbal lock is a singularity condition in which a degree of freedom gets lost such that rotation around one axis has exactly the same effect as rotation around another axis. This problem can also be avoided by adjusting pre-leveled data, simplifying the rotation matrix.

By analytically populating the matrices in (2.9) with (2.7) and its first order Taylor series approximation, a standalone Qt-based C++ program was developed to compute the seven transformation parameters required to match a set of measured data to a corresponding set of control data using the nonlinear least squares method. Qt is an open-source class-based graphical user interface (GUI) extension for C++. See Appendix A for more details on this program and instructions regarding its use.

2.2.3 NISLT – A Least Squares Alternative

The NonIterative Solution to Linear Transformations (NISLT) developed by Han (2010b) from eigentheory has shown promise as a reliable and efficient alternative to the sometimes computationally intensive, nonlinear least squares solution. Rather than simultaneously distributing the overall error evenly between the seven transformation parameters as in least squares, the NISLT technique computes an average scale, rotation, and translation, each independently. This section summarizes the technique itself as presented in Han (2010b). Section 2.2.4 presents optimizations of the technique while Section 2.2.5 contrasts NISLT against least squares.

Given the matrix form of the similarity transformation equation in (2.7), and point coordinates in the vertical vector form of (2.1), scale can be estimated by comparing the distances between all control point combinations to the distances between all original point combinations and taking an average:

$$\hat{s} = \text{mean}\left(\frac{\left\|d\boldsymbol{x}'_{ij}\right\|}{\left\|d\boldsymbol{x}_{ij}\right\|}\right) \ (i \neq j) \tag{2.10}$$

where $\left\|d\boldsymbol{x}_{ij}\right\|$ is the distance between the original points *i* and *j*, and $\left\|d\boldsymbol{x}'_{ij}\right\|$ is the distance between control points *i* and *j*. The rotation matrix $\boldsymbol{R}$ can be estimated using an equation developed through eigentheory:

$$\widehat{\boldsymbol{R}} = \Delta\boldsymbol{X}'^{T}\Delta\boldsymbol{X}_s(\Delta\boldsymbol{X}_s^T\Delta\boldsymbol{X}_s)^{-1} \tag{2.11}$$

where $\Delta \boldsymbol{X}_s$ is formed by stacking the transposed and scaled vectors between the original points and $\Delta \boldsymbol{X}'$ is formed by stacking the transposed vectors between transformed points as shown:

$$\Delta \boldsymbol{X}_s = \hat{s} \begin{bmatrix} d\boldsymbol{x}_{12}^T \\ d\boldsymbol{x}_{13}^T \\ \vdots \\ d\boldsymbol{x}_{ij}^T \end{bmatrix}_{i \neq j} \quad \Delta \boldsymbol{X}' = \begin{bmatrix} d\boldsymbol{x}_{12}'^T \\ d\boldsymbol{x}_{13}'^T \\ \vdots \\ d\boldsymbol{x}_{ij}'^T \end{bmatrix}_{i \neq j} \tag{2.12}$$

Finally, the translation vector can then be estimated by calculating the average shift between the rotated, scaled points and the transformed points:

$$\hat{\boldsymbol{t}}' = mean\left(\boldsymbol{x}' - \hat{s}\hat{\boldsymbol{R}}\boldsymbol{x}\right) \tag{2.13}$$

An implementation of this method using a MATLAB script is presented in Appendix B with instructions for its use.

2.2.4 NISLT Optimization

A simple modification can improve the computational efficiency of the NISLT similarity model. This optimization was implemented in the MATLAB script and discussed in this section.

As defined in the previous section, $d\boldsymbol{x}_{ij}$ will be equal to $-d\boldsymbol{x}_{ji}$ when formulating the matrices—similarly, $d\boldsymbol{x}'_{ij}$ will be equal to $-d\boldsymbol{x}'_{ji}$. Since all terms are equally weighted, computing both $d\boldsymbol{x}_{ij}$ and $d\boldsymbol{x}_{ji}$ (and $d\boldsymbol{x}'_{ij}$ and $d\boldsymbol{x}'_{ji}$) unnecessarily doubles the computations and memory usage in (2.10) and (2.12). Therefore,

these equations can be modified by changing ($i \neq j$) to ($j > i$) where i increments from 1 to n-1, and j increments from i to n, where n is the number of point pairs. This also reduces the number of rows in the matrices $\Delta \boldsymbol{X}_s$ and $\Delta \boldsymbol{X'}$ by half from $n(n-1)$ to $n(n-1)/2$, reducing the required memory to store the matrices and subsequently the computations required for (2.11). For example, in one test run with 19 point pairs, this optimization reduced the dimensions of $\Delta \boldsymbol{X}_s$ and $\Delta \boldsymbol{X}'$ from 342×3 to 171×3, noticeably reducing computation time without altering the final results.

2.2.5 Adjustment Method Comparison

While computation time for the nonlinear least squares method increases exponentially to compute the inverse (a computationally intensive procedure), the NISLT technique increases linearly as the data set size increases, making it very attractive for LiDAR data applications in which data sets can easily number in the millions of points.

A typical way to measure the effectiveness of an adjustment is to calculate the root mean square error (RMSE)

$$RMSE = \sqrt{\frac{\sum_n (x'-x)_i^2 + (y'-y)_i^2 + (z'-z)_i^2}{n}} \tag{2.14}$$

Ten RTK GPS points were collected near the Oregon State University campus and adjusted to control coordinates using the NISLT and traditional least

squares methods. It was observed that two points suffered significantly from multi-path and were removed as outliers for a second comparison. The results of these adjustments are presented in Table 1. Italicized values in Table 1 are the sum of the squares of the corresponding row or column and should always equal exactly 1, according to Property 3 listed in Section 2.1.1.

When (2.5) was used to extract roll, pitch, and yaw from the rotation matrices, the results from $\widehat{\boldsymbol{R}}$ were significantly different from the results of a traditional least squares solution (as shown in Table 2). ***R-calc*** in Table 1 was computed with (2.4) from the roll, pitch, and yaw values extracted from $\widehat{\boldsymbol{R}}$, resulting in very poor RMSE values, especially with outliers present.

R-mod was computed numerically using a spreadsheet to simulate a NISLT solution of (2.11) constrained by the six conditions in (2.6) in an attempt to force the properties of a rotation matrix onto $\widehat{\boldsymbol{R}}$. The six constraints counteracted the six additional unknowns introduced by solving for the nine elements of $\boldsymbol{R}$ instead of the three rotation angles, granting the numerical solution the same degree of freedom as a traditional least squares solution.

Table 1: Comparison of 3x3 rotation matrices from different adjustment methods for a set of GPS points, with and without outliers. Italicized values are the sum of the squares of the corresponding row or column.

10-Point Solution (with outliers)				8-Point Solution (without outliers)			
$\widehat{R}$ (RMSE 0.1117)				$\widehat{R}$ (RMSE 0.0196)			
0.40628	-0.91328	-0.03713	*1.00052*	0.40820	-0.91438	0.06065	*1.00639*
0.90952	0.41107	-0.16295	*1.02275*	0.91335	0.40780	0.00846	*1.00058*
-0.01528	0.01458	0.31532	*0.09987*	-0.00037	0.00125	0.94026	*0.88409*
0.99252	*1.00327*	*0.12736*		*1.00084*	*1.00238*	*0.88784*	
R-calc (RMSE 1.0565)				***R-calc*** (RMSE 0.0416)			
0.40781	-0.91178	0.04843	*1.00000*	0.40803	-0.91297	0.00137	*1.00000*
0.91294	0.40807	-0.00486	*1.00000*	0.91297	0.40803	-0.00021	*1.00000*
-0.01534	0.04620	0.99882	*1.00000*	-0.00037	0.00133	1.00000	*1.00000*
1.00000	*1.00000*	*1.00000*		*1.00000*	*1.00000*	*1.00000*	
R-mod (RMSE 0.1304)				***R-mod*** (RMSE 0.0233)			
0.40728	-0.91330	-0.00408	*1.00000*	0.40791	-0.91302	-0.00023	*1.00000*
0.91329	0.40730	-0.00350	*1.00000*	0.91302	0.40791	0.00067	*1.00000*
-0.00527	-0.00102	0.99999	*1.00000*	0.00008	-0.00012	1.00000	*1.00000*
1.00000	*1.00000*	*1.00000*		*1.00000*	*1.00000*	*1.00000*	
R-LS (RMSE 0.1292)				***R-LS*** (RMSE 0.0221)			
0.40688	-0.91348	0.00123	*1.00000*	0.40788	-0.91304	-0.00033	*1.00000*
0.91346	0.40689	0.00529	*1.00000*	0.91304	0.40788	-0.00054	*1.00000*
-0.00533	-0.00103	0.99999	*1.00000*	0.00063	-0.00008	1.00000	*1.00000*
1.00000	*1.00000*	*1.00000*		*1.00000*	*1.00000*	*1.00000*	

Table 2: Comparison of roll, pitch, and yaw values derived from rotation matrices produced by different adjustments, with and without outliers.

	10-Point Solution			8-Point Solution		
	$\widehat{R}$	***R-mod***	***R-LS***	$\widehat{R}$	***R-mod***	***R-LS***
Roll (°)	-2.6481	0.0583	0.0591	-0.0764	0.0069	0.0046
Pitch (°)	-0.8787	-0.3022	-0.3053	-0.0213	0.0045	0.0359
Yaw (°)	-65.9298	-65.9657	-65.9904	-65.9189	-65.9261	-65.9283

2.3 TRANSFORMATION AND ADJUSTMENT CONCLUSIONS

Han (2010b) demonstrated that the NISLT technique could be reliable for high-precision synthetic data, producing results similar to traditional least squares methods in a fraction of the time. Nevertheless, caution should be exercised while using the results of the NISLT technique because rotation matrix properties are not conserved.

It is interesting to note that the RMSE reported using $\widehat{\boldsymbol{R}}$ is lower than the least squares adjustment (***R-LS***), which should, by definition, produce the result with the theoretical minimum RMSE. The rotation matrix approximation $\widehat{\boldsymbol{R}}$ does not demonstrate Property 3 of a rotation matrix (Section 2.1.1) and is therefore not a true rotation matrix. This is likely because the NISLT technique solves for the nine elements of the rotation matrix as nine independent variables, when, in fact, a rotation matrix consists of nine dependent variables calculated from three independent angles (roll, pitch, and yaw). This increased number of degrees of freedom may explain why the RMSE using $\widehat{\boldsymbol{R}}$ appears to be lower than what would be theoretically possible.

The discrepancy between $\widehat{\boldsymbol{R}}$ and ***R-calc*** has two very important implications. Firstly, a user of the NISLT technique cannot rely on the extracted roll, pitch and raw as implied by Han (2010b), but should use $\widehat{\boldsymbol{R}}$ directly in all subsequent computations. Secondly, the NISLT in its present form appears to be more

sensitive to outliers than traditional least squares methods, but more research using poor-quality data is recommended to further evaluate this.

While the ***R-mod*** solution was very slow compared to ***R-LS*** and $\widehat{\boldsymbol{R}}$, its low RMSE and rotation angles comparable to ***R-LS*** demonstrate that an analytical application of one constraint to the NISLT technique could theoretically maintain the advantages of the NISLT technique while overcoming its shortcomings. To the author's knowledge, no such analytical solution has yet been found.

3 MANUSCRIPT CHAPTER

To Level or Not to Level:

Laser scanner inclination sensor accuracy evaluation

Evon P. Silvia[1] and Michael J. Olsen[2]

1. Graduate Assistant, School of Civil and Construction Engineering, Oregon State University, 220 Owen Hall, Corvallis, OR, 97331, evon.silvia@gmail.com
2. M.ASCE. Assistant Professor, School of Civil and Construction Engineering, Oregon State University, 220 Owen Hall, Corvallis, OR, 97331, michael.olsen@oregonstate.edu

ASCE Journal of Surveying Engineering

http://ascelibrary.org/suo/

Manuscript under review. Submitted on April 12, 2011 (Manuscript #SUENG-191).

3.1 ABSTRACT

Many modern terrestrial laser scanners (TLSs) are equipped with inclination/tilt sensors—also referred to as level compensators—that can correct out-of-level imperfections in an instrument setup. Some users elect to disable the inclination sensor when their scanner is equipped with one. Those who do use an inclination sensor may override its leveling data by linking to external control that defines the level plane. Our case study has shown that inclination sensor data can be a valuable quality check on the control data and overall point cloud alignment. Rigorous testing revealed that caution must be exercised in scan planning to ensure quality inclination sensor data. Specifically, lab tests indicate that scanner rotation speed influences the reliability of inclination sensor readings recorded during rotation. These inertial effects can be cancelled to a limited extent by measuring during both clockwise and counter-clockwise rotations. A scan duration within a “stability threshold” can also minimize the inertial effects and variability in inclination sensor readings for scanners continuously measuring inclination data during rotation. Finally, inclination sensor readings from a full 360° rotation are recommended to reduce systematic bias.

3.2 INTRODUCTION

Terrestrial laser scanners (TLS) continue to grow in popularity as increasingly more applications are discovered. Vosselman and Maas (2010) present a detailed overview of TLS and airborne laser scanning technology, related errors, potential applications, and data processing techniques, while Wehr and Lohr (1999) provide an overview of laser scanning in general.

As the TLS industry develops, it will likely continue to become less expensive while enabling more rapid data acquisition, following the trend already seen in airborne laser scanning (Wynne 2006). Although scan point clouds are undeniably impressive to both the casual observer and geomatics professional, TLS technology is still in its infancy and thus its precision and accuracy still require evaluation. These studies are particularly important given the complexity of error sources native to laser scanning. Attention to TLS error and calibration has increased with developments in the technology (Lichti 2007), emphasizing impacts from angular displacement, mixed pixels, detector saturation, blooming, multipath, and incidence angle (Lichti, Gordon and Tipdecho 2005). Efforts to produce standardized accuracy tests for TLS are ongoing in multiple contexts, including ISO standards (Cuartero, et al. 2010), manufacturer-independent instrument comparisons (Mechelke, Kersten and Lindstaedt 2007), cultural heritage scanning (Boehler, Vicent and Marbs

2004), construction standards (Ravani, et al. 2007), and self-calibration (Lichti 2007; Lichti and Licht 2006).

3.2.1 Scan Registration

Further advancement of TLS technology in recent years has included improvements in scan alignment techniques. Registration of scans to targets setup at known or externally measured positions is a common method for TLS alignment. However, safety and time constraints can make target registration impractical, leading to the development of other registration techniques. Three example situations and solutions are:

- Construction and underground mining sites operate on tight schedules that must minimize interruptions and cost. Operation of dual-axis inclination sensors enables faster setup by requiring fewer targets for scan registration (Ravani, et al. 2007), reducing the cost of replacing targets disturbed during the construction process and reducing the safety risks associated with target placement without losing accuracy.
- Cliff and landslide monitoring applications make the use of targets a safety risk to field crews. The iterative closest point technique (ICP) originally developed primarily by (Besl and McKay 1992) has seen many developments in recent years, including in the context of laser scanning. This software-based technique uses common surface

features possessing distinct geometry to match scans to a reference scan without the use of targets. For a summary of modern applications of and improvements to ICP, see Vosselman and Maas (2010) and Salvi, et al. (2007).

- Attempting to scan large geographic areas using TLS presents unique challenges, including the need to quickly georeference data to a real-world coordinate system. A surface matching, azimuth adjustment technique (Olsen, et al. 2009, 2011) has been shown to produce repeatable results within equipment specifications, particularly over long coastal sections. This technique determines scanner origin coordinates using RTK GPS, constrains scans to level using inclination sensors, and conducts a software adjustment to the azimuth using a point to plane ICP variant based on matching features common to multiple adjacent scans.

Some of these techniques require the field data to be close to level for reliable and efficient operation. Field procedures and time constraints can inhibit exact instrument leveling at every setup, and so many TLS manufacturers have provided means to compensate for unlevel setups, both in the instrument itself and in accompanying software. As dependence upon proper compensation increases, so must the scrutiny of these devices.

3.2.2 Inclination Sensors

Most modern laser scanners now have inclination sensors (JADA Productions 2010), also referred to as level compensators, inclinometers, or tilt sensors. For clarity, we will refer to them herein solely as inclination sensors.

Given a right handed scanner coordinate system with the *X* axis pointing along the scanner's initial line of sight, the *Y* axis at 90° counter-clockwise from the *X* axis in the horizontal plane, and the *Z* axis pointing vertically upwards, rotation of the scan setup into a project coordinate system (*X'*, *Y'*, *Z'*) is usually described in terms of roll (α), pitch (β), and yaw (γ) as rotations around the *X*, *Y*, and *Z* axes, respectively. Note that these three rotations can also be summarized as a single rotation about a single vector (quaternion). Inclination sensors measure roll and pitch of the instrument, while yaw is related to the scanner's bearing or azimuth relative to an external project coordinate system.

Given a laser scan data point, $\boldsymbol{P_0}$, with coordinates (*X*, *Y*, *Z*), alignment adjustments can be applied by rotating the point around the *X*, *Y*, and *Z* axes centered at the scan origin:

$$\boldsymbol{P'} = \boldsymbol{R_z R_y R_x P_0} \tag{3.1}$$

$$\boldsymbol{P'} = \boldsymbol{R}(\alpha, \beta, \gamma)\boldsymbol{P_0} \tag{3.2}$$

$$\boldsymbol{R}(\alpha,\beta,\gamma) =$$

$$\begin{bmatrix} \cos\beta\cos\gamma & \cos\alpha\sin\gamma+\sin\alpha\sin\beta\cos\gamma & \sin\alpha\sin\gamma-\cos\alpha\sin\beta\cos\gamma \\ -\cos\beta\sin\gamma & \cos\alpha\cos\gamma-\sin\alpha\sin\beta\sin\gamma & \sin\alpha\cos\gamma+\cos\alpha\sin\beta\sin\gamma \\ \sin\beta & -\sin\alpha\cos\beta & \cos\alpha\cos\beta \end{bmatrix} \quad (3.3)$$

Where $\boldsymbol{R_z}$, $\boldsymbol{R_y}$, and $\boldsymbol{R_z}$ are the rotation matrices around each individual axis, $\boldsymbol{R}$ is the combined rotation matrix around the scan origin, and $\boldsymbol{P'}$ is a vector of the point coordinates in the new coordinate system. Note that a translation along *X'*, *Y'*, and *Z'* needs to be performed after rotation for complete registration. When applying only level corrections, $\boldsymbol{R_z}$ would be an identity matrix and γ would be zero, simplifying $\boldsymbol{R}$.

Note that unlike airborne or mobile systems where a level correction is normally applied on a point per point basis through the use of an inertial motion unit (IMU), TLS level corrections are ordinarily applied to an entire setup with the assumption that the scanner platform is static. Hence, every scan and every point recorded at a particular setup receives the same correction.

3.2.3 Survey of TLS Professionals

The Oregon State University geomatics program conducted a brief online survey of laser scanning professionals in September, 2010 (see results in Appendix D). The intent of the survey was not to be a rigorous scientific survey, but rather to evaluate the industry's use and understanding of TLS

inclination sensors and applications. 81% of the 48 respondents indicated that their scanners were equipped with an inclination sensor and 69% of the 48 respondents used it all or most of the time. The survey results generally indicated an informed understanding of the scanner's inclination sensor and its uses. Many TLS professionals who use inclination sensors stated that they rely on their level data to provide additional control, reducing field time required to set up additional targets, thereby simplifying scan registration to an existing coordinate system (georeferencing). The most common complaint regarding inclination sensors was that their use significantly increased scan time for certain scanner models, which explains why some users choose not to always have them enabled.

3.2.4 Scope of Manuscript

Due to their established presence in the context of land surveying, inclination sensor applications in TLS and related error have not been heavily researched. Inclination sensor error is generally assumed to behave similarly to what has been shown with digital levels, theodolites, and total stations—*i.e.*, it is entirely a function of plate bubble sensitivity (Lichti, Gordon and Tipdecho 2005) and calibration error (Mechelke, Kersten and Lindstaedt 2007) when the error is small. Large leveling errors are generally attributed to environmental instability, modeling biases, and scanner resolution, in addition to the TLS errors previously listed. Additionally, several scanners operate at close ranges

(<100 m), reducing the impact of slightly unlevel data. However, for scanners that can acquire data at longer ranges (>1 km), inclination sensors become increasingly important to ensure data accuracy (Wehr and Lohr 1999).

While the function of inclination sensors in TLS and total stations may be conceptually similar, their uses (as described above in the Scan Registration section) and implementation in TLS are far more complex. In the case of a total station, the instrument remains static during each discrete point measurement. However, many TLS systems simultaneously rotate and record thousands of points in the same amount of time as a single point from a total station. This manuscript will show that this distinction between static and dynamic inclination data collection is significant, particularly since some high speed laser scanners allow setups as much as 15 degrees off center to be corrected to level, whereas total stations normally force a near-level setup prior to data acquisition. Additionally, because of the wide variety of applications for TLS, scans may be collected by individuals without a surveying background who may not understand the implications of data being out of level.

This manuscript presents an analysis of the impact of scanner rotation speed on inclination sensor results from several test procedures. Additionally, a case study undertaken at the Hinsdale Wave Research Laboratory at Oregon State

University that demonstrates the value of quality inclination sensor data is also presented.

3.3 INCLINATION SENSOR ACCURACY STUDY

As described above in the introductory sections of this paper and will be demonstrated in the case study presented in the next section, TLS inclination sensors have significant value as a quality control and scan registration tool. While manufacturers often list precision specifications for a sensor in a particular instrument, these sensors occasionally show more variability in actual operation than during strictly controlled testing. This led to an investigation into one probable cause: inertial disturbance from scanner rotation during readings.

3.3.1 Review of TLS Inclination Sensors

How each scanner measures inclination sensor data varies with manufacturer, and data storage and extraction occur within a “black box” from the end user’s perspective. Table 3 summarizes inclination sensors for some modern scanners.

Table 3: Summary of inclination sensor measurement techniques of four example scanners. Modified from JADA Productions 2010; FARO Technologies Inc. 2009; and Leica Geosystems AG 2011.

Scanner Model	Inclination Sensor Measurement	Inclination Sensor Range (from horizontal plane), Resolution, and Precision (1-sigma)
FARO LS 880	Continuous, after scan, while recording photographs	Range: ± 15° Resolution: 3.6” Precision: 6.3”
Leica ScanStation 2 and C10	Incremental, pausing to measure for each vertical scan line. If significant changes are detected, the scan is aborted. (automatic)	Range: ± 0.083° Resolution: 1” Precision: 1.5”
Maptek I-Site 8800	Performs leveling analysis during a continuous, 1 minute, 360° preview cycle prior to scan acquisition.	Range: ± 5° Resolution: 20” Precision: unlisted
Riegl VZ-400 (other models similar)	(1) Continuous during scan (automatic) (2) Discrete, 360° rotation, pausing every 60° for 1 second to measure (semi-automatic) (3) Continuous, both clockwise and counter-clockwise (semi-automatic)	Range: ± 10° Resolution: 3.6” Precision: 0.5”

TLS specifications should include some statement regarding the precision of its built-in inclination sensor—the Riegl VZ-400 used in this study lists its one-sigma value at ±0.008 degrees, or 28.8 seconds. Like most laser scanner specifications, the exact procedure used to determine these values appears to vary from manufacturer to manufacturer and comparing scanners can be difficult, though some work has been done to develop a common basis for comparison (Mechelke, Kersten and Lindstaedt 2007).

3.3.2 Problem Statement

From the comments given in the industry survey described previously, there appears to be a tacit assumption in the industry that inclination sensors in laser scanners behave similarly to those found in total stations. However, to reduce scan durations, many new scanners simultaneously acquire point data and level corrections. That is, unlike total station operation, the inclination sensors in these newer scanners are not static while measurements are taken.

In the case of a rotating scanner head, if the inclination sensor is not located precisely in the center of rotation (a near-impossible feat given that many scanners can be set up out of level), then it would follow intuitively that while inclination sensors can stabilize during slow scans, inclination sensors would be unable to reach vertical equilibrium during fast scans. That stability threshold where the inclination sensor achieves near equilibrium prior to measurement must be determined for each scanner.

The following sections describe an investigation into the existence of such a threshold and other factors contributing to inclination sensor error. Please note that roll and pitch described throughout this section are measured relative to the fixed scanner reference frame, not the scanner head orientation at the time of measurement.

3.3.3 Stability Threshold Evaluation

The purpose of this evaluation was two-fold: (1) to verify a correlation between scanner rotation speed and inclination sensor stability, and (2) to develop a methodology to determine a minimum recommended scan duration that ensures the stability of the inclination sensor—that is, a *stability threshold* for the inclination sensor. This test was intended to be straightforward enough to determine the stability threshold of any similar scanner.

3.3.3.1 Stability threshold evaluation methodology

The evaluation involved two independent setups: one carefully leveled and the other intentionally out of level to determine whether the magnitude of inclination measurements amplified any speed-related effects observed. Nine 360° scans were collected from each setup at scan speeds ranging from 6 seconds to 740 seconds. Past experience with the scanner suggested that the stability threshold was likely in the range of 60 to 400 seconds, so the test emphasized speeds around that range, which may vary between scanners.

Retro-reflective targets with known coordinates were distributed throughout the room and scanned at the beginning of each setup to provide reliable external control for evaluating inclination sensor accuracy. Coordinates for these control targets were defined using a carefully leveled Leica TCRP 1201+ survey grade total station.

In order to demonstrate that results were not peculiar to the inclination sensor in the scanner used for this study and that it was consistent with itself, the discrete inclination measurement feature described as VZ-400 method (2) in Table 3 was used to record static inclination data after the scans were completed. This “discrete method” resembles inclination sensor data collection from other scanner models that pause rotation while acquiring scan data.

Significant efforts were undertaken to reduce external errors sources during and between scans. Solid connections between the scanner and tripod components restricted undesired rotation of the scanner. Rather than using the keypad on the scanner head itself, the instrument was operated remotely from a wireless laptop to eliminate any disturbances introduced by pressing buttons on the scanner head and having cables hanging from the scanner. Once setup was completed, no contact was made with the scanner head for the duration of each setup.

3.3.3.2 Stability threshold results and discussion

The results of the evaluation are presented in Table 4 and Figure 4. The data show a significant shift between the 30-second scan and the 6-second scan in the Leveled setup that skews the data. This extreme variability of inclination values from the 6-second scan had been observed during previous scans, so rather than removing it as an outlier, it seemed fitting to retain the data to

demonstrate the risk associated with using inclination sensor readings obtained during extremely fast scans.

The inclination values computed from a registration to external control is provided in the tiepoint (TP) registration row. Discrete method (DM) and software (SW) residuals were computed against the TP average and found to converge toward zero as the scan duration increased.

Table 4: Test 2 results for 360° scans from both unlevel and level scans. "DM" = roll and pitch values measured using the discrete method described in Table 3. "SW" = roll and pitch values extracted from the raw scan data using the scanner's accompanying software.

NOT LEVELED									
Time Elapsed	Resolution	Roll (°)				Pitch (°)			
(sec)	(°)	DM	DM res.	SW	SW res.	DM	DM res.	SW	SW res.
740	0.02	-0.723	-0.002	-0.723	-0.002	-1.686	0.010	-1.690	0.006
475	0.025	-0.714	0.007	-0.719	0.002	-1.691	0.005	-1.691	0.005
330	0.03	-0.715	0.006	-0.720	0.001	-1.716	-0.020	-1.692	0.004
185	0.04	-0.717	0.004	-0.722	-0.001	-1.687	0.009	-1.691	0.005
83	0.06	-0.714	0.007	-0.721	0.000	-1.686	0.010	-1.688	0.008
52	0.076	-0.722	-0.001	-0.723	-0.002	-1.676	0.020	-1.686	0.010
47	0.08	-0.718	0.003	-0.703	0.018	-1.695	0.001	-1.714	-0.018
30	0.09875	-0.734	-0.013	-0.652	0.069	-1.675	0.021	-1.713	-0.017
6	v0.1°, h0.5°	-0.734	-0.013	-0.728	-0.007	-1.646	0.050	-1.709	-0.013
average		-0.721		-0.712		-1.684		-1.697	
standard deviation		0.008		0.024		0.019		0.011	
tiepoint registration				-0.721				-1.696	
LEVELED									
Time Elapsed	Resolution	Roll (°)				Pitch (°)			
(sec)	(°)	DM	DM res.	SW	SW res.	DM	DM res.	SW	SW res.
740	0.02	-0.014	-0.009	-0.006	-0.001	-0.022	0.018	-0.037	0.003
475	0.025	0.006	0.011	-0.006	-0.001	-0.047	-0.007	-0.036	0.004
330	0.03	0.004	0.009	-0.007	-0.002	-0.047	-0.007	-0.036	0.004
185	0.04	-0.013	-0.008	-0.009	-0.004	-0.032	0.008	-0.033	0.007
83	0.06	0.023	0.028	0.001	0.006	-0.047	-0.007	-0.038	0.002
53	0.075	no data	—	-0.014	-0.009	no data	—	-0.050	-0.010
47	0.08	-0.013	-0.008	0.001	0.006	-0.038	0.002	-0.062	-0.022
30	0.09875	-0.003	0.002	0.029	0.034	-0.026	0.014	-0.041	-0.001
6	v0.1°, h0.5°	0.004	0.009	0.212	0.217	-0.054	-0.014	0.497	0.537
average		-0.001		0.022		-0.039		0.018	
standard deviation		0.013		0.072		0.011		0.180	
tiepoint registration				-0.005				-0.040	

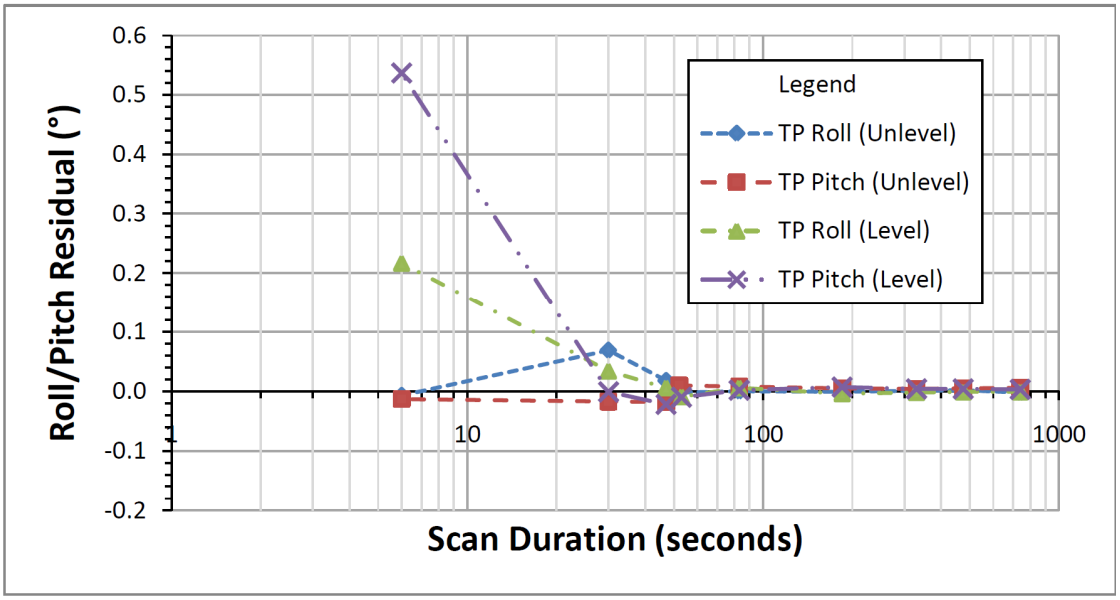

Figure 4: Test 2 plot of TP residuals computed from tiepoint registration against scan duration on a logarithmic scale. Note that all four plots appear to converge to zero at approximately 83 seconds.

It had been observed in previous versions of this test that the simple act of nudging the power cable resulted in instantaneous variations of roll and pitch by as much as ±0.10°. By operating the instrument remotely and eliminating all physical contact with the scanner upon setup completion, the scans were noticeably more consistent for each setup, significantly reducing the overall standard deviation.

The significant discrepancy in the overview scan data for the leveled setup may appear suspicious, but it accurately demonstrates the variability observed in inclination data derived from extremely fast scans (as shown in the following section). Because of the skew this introduces to the un-weighted average, an

average was also computed for each setup from the five slowest scans that was almost identical to the averaged DM results and the TP results, suggesting that under the right conditions the inclination sensor is precise and accurate, respectively, within the standard deviation provided in the specifications.

From Figure 4 it can be seen that inclination data extracted from a scan with a duration of at least 100 seconds should be reliable for the scanner used in this study. This stability threshold will likely vary from scanner to scanner, but the same procedure can be used to determine it.

3.3.4 Rotation Speed Effects

While the stability threshold appears to be correlated with scan duration, it remains to be demonstrated that this effect is actually a function of scan speed and not some other factor—for example, the roll and pitch values such as those presented in the previous section are usually a simple average computed over the duration of the scan, and so a smaller sample size in shorter scans may simply be statistically less reliable.

3.3.4.1 Rotation speed comparison methodology

Full 360° scans of durations of approximately 0.1 minutes, 0.5 minutes, 1 minute, 3 minutes, 5 minutes, and 10 minutes were recorded in a controlled lab setting from a single, stable, unlevel scan setup. As observed in the

stability threshold evaluation, the same effects were observed regardless of whether or not the setup was carefully leveled. Every scan was recorded in the clockwise direction.

These particular scan durations were selected because they straddled the stability threshold determined in the previous section. Thus, measurements from scans above the stability threshold should show statistically the same variability, while measurements from scans below the stability threshold should show higher variability.

Individual inclination measurements were extracted from each scan's raw measurement data. As before, roll and pitch described throughout this section are shown relative to the fixed scanner reference frame, not the scanner head orientation at the time of measurement.

3.3.4.2 Rotation speed comparison results and discussion

Figure 5 shows radial plots of roll (top) and pitch (bottom) from four of the six scans recorded. The two longer scans showed the same tendencies as the 3-minute scan and were excluded from the plots for clarity. A perfect circle with minimal noise would indicate a constant and extremely stable inclination measurement. The inclination sensor used in this study was very sensitive to environmental disturbances, including nearby slammed doors and passing trucks, which is evident in the sudden spike around 190° for the 3-minute plot.

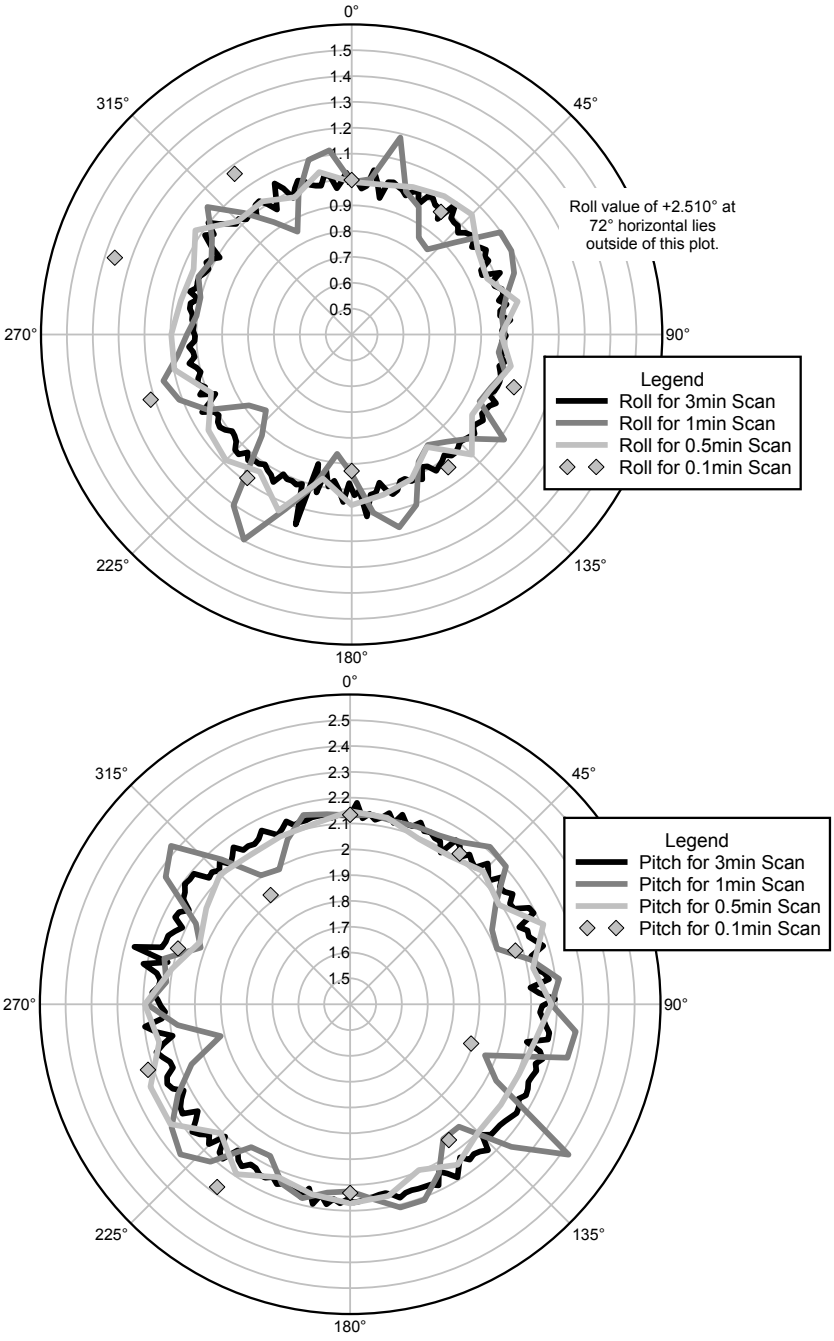

Figure 5: Radial plots of roll (top) and pitch (bottom) measurements (radial axis, in degrees from level) at approximate horizontal scanner head rotation positions (polar axis). Scan durations listed are approximate. Measurements were taken approximately once per second.

As expected, individual measurements from scans with durations shorter than this scanner's stability threshold of 100 seconds generally show higher variability from a perfect circle than longer scans (Figure 5). This indicates a direct correlation between scan rotation speed and error amplitude for an individual measurement, which is confirmed by a computation of the standard deviations of each scan.

3.3.5 Scanner Position Effects

Intuitively one would assume that inclination data from a 360° scan would be more representative of the overall scan setup than a scan that, for example, only recorded in a scan window from 120° to 180°. To verify this, average roll and pitch inclination values were computed from 60° subsets of the 3-minute scan from the previous section. Results for each interval varied from the overall average by up to ±0.02° for both roll and pitch. This difference can be significant, as the difference between +0.02° and -0.02° translates to a vertical offset of approximately 3.5 cm at 50 m.

It should also be noted that there was some variability observed in initial measurements due to scanner park position, which is the rotating scanner head's resting position relative to the position where it begins measurements. These effects were removed in the scans shown by making the park position and start position identical.

3.3.6 Scanner Directional Effects

Now that it has been shown that the inertial effects observed in inclination data recorded during scan rotation increase with rotation speed, it is possible that this error can be partially or completely mitigated by recording inclination data in both clockwise and counter-clockwise directions. If the inertial error is systematic, it should theoretically cancel out if inclination data is recorded in both rotational directions.

3.3.6.1 Scanner directional effects assessment methodology

Twenty 6-second 360° overview scans were recorded from a moderately unlevel setup, alternating clockwise and counter-clockwise such that ten were recorded in a clockwise direction and ten were recorded in a counter-clockwise direction. The raw inclination data from each scan was software-extracted and averaged. Inclination data was also measured from the same setup using the semi-automatic Riegl VZ-400 inclination measurement methods described in Table 3.

3.3.6.2 Scanner directional effects assessment results and discussion

The results of the three sets of tests are summarized in Table 5. “Scans (all)” represents the combination of 20 scans. “Scans (paired)” was generated by averaging the 10 pairs of consecutive clockwise and counter-clockwise scans.

"Scans (cw only)" represents only the 10 clockwise scans, while "Scans (ccw only)" represents only the 10 counter-clockwise scans. "Discrete" represents a set of 20 measurements using method (2) from Table 3. "Continuous" represents a set of 20 measurements using method (3) from Table 3.

Table 5: Comparison of inclination measurement methods, in degrees. "cw" = clockwise and "ccw" = counter-clockwise.

Method		Average	StDev	Range
Scans (all)	Roll	0.753	0.103	0.379
	Pitch	0.826	0.043	0.133
Scans (paired)	Roll	0.753	0.049	0.171
	Pitch	0.826	0.013	0.036
Scans (cw only)	Roll	0.823	0.073	0.246
	Pitch	0.790	0.014	0.042
Scans (ccw only)	Roll	0.683	0.078	0.188
	Pitch	0.862	0.026	0.075
Discrete	Roll	0.789	0.007	0.027
	Pitch	0.823	0.008	0.034
Continuous	Roll	0.787	0.005	0.017
	Pitch	0.815	0.001	0.003

As shown in Table 5, clockwise measurements consistently measured roll significantly higher than the average, while counter-clockwise measurements were low. The pitch values showed the opposite pattern, but with less consistency. Pairing and averaging the clockwise and counter-clockwise scans into ten sets of two scans improved the standard deviations and range of both roll and pitch by at least a factor of two. This suggests that inertial effects can be reduced by performing scans in both the clockwise and counter-clockwise directions for inclination data recorded at high speeds. Recall that the listed

one-sigma value of the instrument used in this study was ±0.008°—scan-measured values consistently showed a standard deviation much higher than that value, especially for roll.

The discrete and continuous inclination measurement methods were conducted separately from the scans, such that the only movement during these measurements was the rotation of the scanner head. The raw data of these methods is not available to the user, as these proprietary methods simply provide roll and pitch values upon completion. Although both methods produced results matching or improving upon the listed precision, the continuous method gave the most consistent results, despite the fact that the scanner head rotation speed during this method is similar to that of a 6-second overview scan. Recall from Table 3 that the continuous method, like the paired-scan method, measures in both clockwise and counter-clockwise directions; if the degradation of inclination data was from scanner rotation speed alone the two methods should have produced similar results. This suggests that another factor introduces random error during laser scanning that is not present when measuring inclination data alone—the rotation of the faceted mirror, possibly.

Nevertheless, it has been confirmed that measuring inclination data in both the clockwise and counter-clockwise directions noticeably improves the quality

and reliability of inclination data, even for extremely fast scans where the error would be most noticeable.

3.4 Case Study: O. H. Hinsdale Wave Research Laboratory

The value of inclination sensors' use in the field is shown through the following case study. In June of 2010, researchers at the O. H. Hinsdale Wave Research Laboratory (HWRL) in Corvallis, Oregon, (Figure 6) requested that the Oregon State University geomatics group perform laser scanning for a 3D record of their scale models tested in the tsunami wave basin.

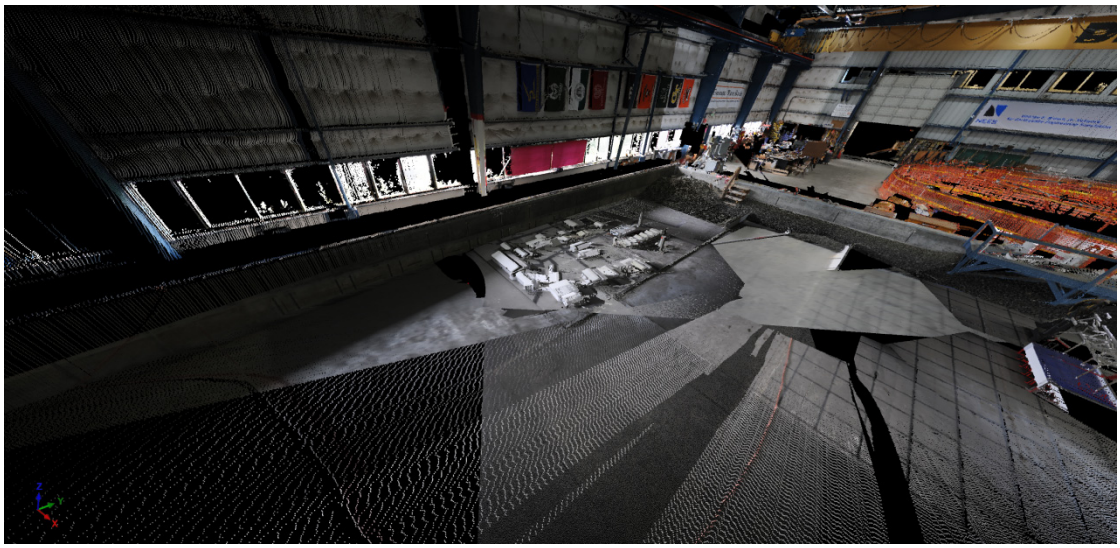

Figure 6: A view of the scan data collected from three scan positions at the O.H. Hinsdale Wave Research Lab (HWRL) tsunami wave basin (TWB) in Corvallis, Oregon. In the center of the figure is a scale model of Cannon Beach, Oregon located in the southwest corner of the TWB.

3.4.1 Background

The HWRL tsunami wave basin is a large facility used for modeling coastal environments and simulating wave events and impacts. Occupying a space approximately 49m x 27m x 2m (160ft x 87ft x 7ft), the basin hosts large constructed scale models that must be properly recorded before and after testing. Baseline scans and surveys of the basin itself were previously conducted by a 3D scanning firm to establish a local coordinate system anchored by three existing, stable benchmarks on the facility floor. Wall targets were surveyed (see Figure 7 for a typical target scan and photograph) to provide convenient tiepoints that could be used to orient and locate subsequent models.

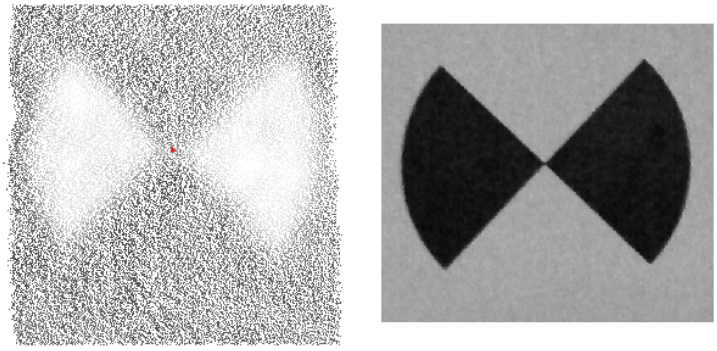

Figure 7: A typical HWRL target colored by return signal amplitude (left) and a grayscale photograph of the same target (right).

Unfortunately, this control proved to be unreliable and the lab manager reported difficulties properly closing surveys and linking data.

3.4.2 Procedure

For this case study, scans were taken in the positions shown in Figure 8, distributed around the wave basin (denoted by the shaded area), focusing on the southwest corner of the wave basin, which was the location of the scale building models being studied. Precise leveling was not performed with each setup, although inclination sensor data was recorded for each scan. No new control or targets were placed for these scans because three to five targets were visible from each scan setup, a sufficient number for registration.

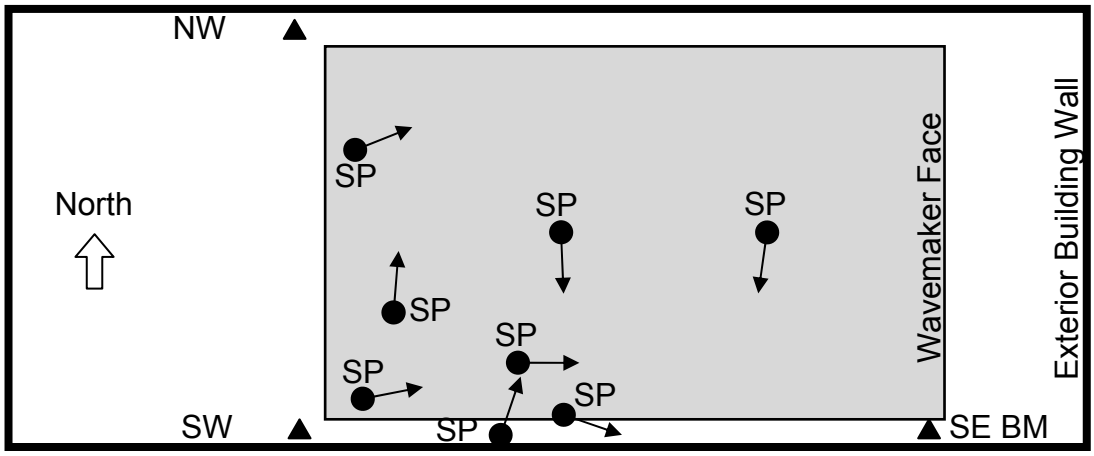

Figure 8: The HWRL tsunami wave basin—building walls are outlined; the wave basin itself is shaded. Scan positions are denoted "SP" with an arrow indicating setup orientation. Brass floor benchmarks are denoted "BM."

3.4.3 Analysis

Scan positions 1, 3, 5, 7, and 8 (Set 1) were registered to the existing local coordinate system using the established targets along the lab walls. To reduce

field time and because the dataset was also going to be used as a training dataset for processing, it was intended to register scan positions 2, 4, and 6 (Set 2) to Set 1 using a level-constrained ICP software alignment. While the standard deviations were acceptable (on the order of 2-4 mm) for the target registration of Set 1, surface matching of Set 2 to Set 1 proved unsatisfactory.

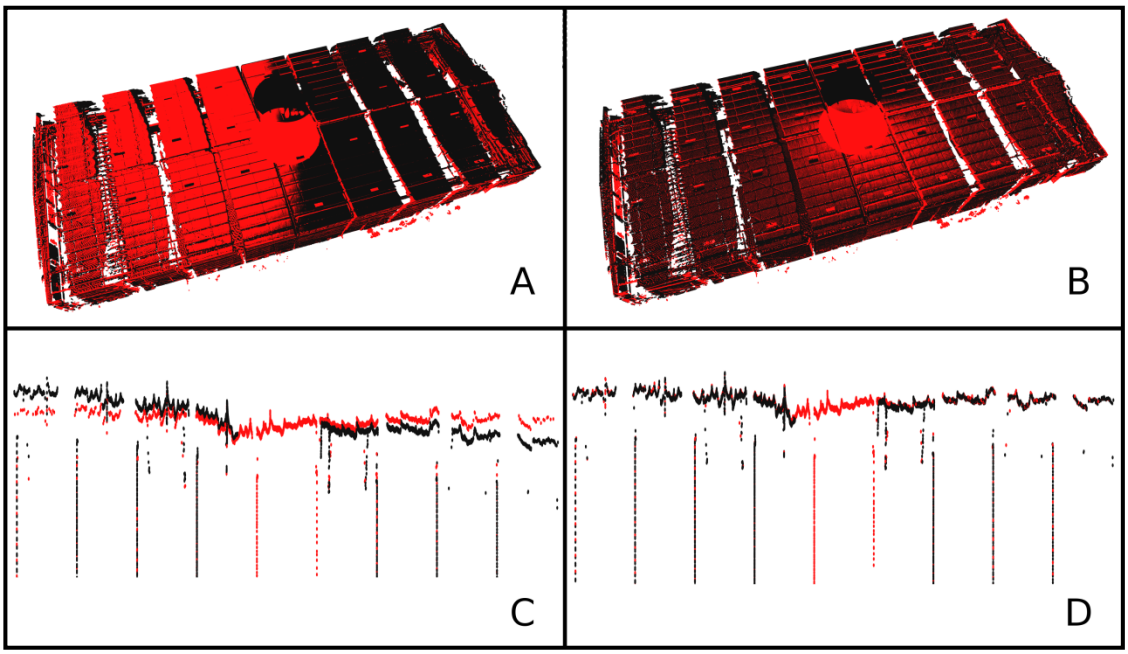

Figure 9: Representative iso-views and cross sections (40x vertical exaggeration) of the wave lab roof after surface registration of scan position 2 (light/red) to scan position 7 (dark/black). Scan position 2 is approximately 7cm below scan position 7 on the west end and 7cm above it on the east end as shown in (A) and (C). Once the control had been corrected, the scans aligned properly as shown in (B) and (D).

Further investigation revealed a consistent directional bias as demonstrated in Figure 9A and C, indicating a problem with the control rather than a problem with scanner accuracy. A comparison of Set 1 roll and pitch values before and

after registration is shown in Table 6. Results indicated a consistent rotation around the north-south axis of approximately 0.12 degrees from level.

Table 6: Comparison of inclination data from inclination sensors compared to post-registration orientation. Inclination sensor data was extracted from overview scans recorded in a 360° window for the specified duration. Results indicate a dominant 0.12° rotation around the north-south axis.

SP	Inclination			Tiepoints			Δ			Axial Rotations	
	Roll (°)	Pitch (°)	Duration (s)	Roll (°)	Pitch (°)	SD (m)	Roll (°)	Pitch (°)	Yaw (°)	E-W (°)	N-S (°)
1	0.396	0.933	53	0.398	0.804	0.0023	0.002	-0.129	168.249	-0.024	0.127
3	-0.061	-0.203	53	-0.181	-0.215	0.0030	-0.120	-0.012	-94.252	0.003	0.121
5	-0.712	0.042	53	-0.823	0.004	0.0031	-0.111	-0.038	-115.065	-0.013	0.117
7	-0.021	-0.070	185	0.106	-0.063	0.0039	0.127	0.007	88.415	0.003	0.127
8	-0.308	0.118	185	-0.347	0.001	0.0020	-0.039	-0.117	-157.585	0.009	0.123
									Average	**-0.004**	**0.123**
									SD	**0.014**	**0.004**

To ensure that the scan inclination readings were correct and that the problem was inherent to the control, the team returned to the site with a survey-grade total station to verify the relative positions of the benchmarks and TLS targets, as well as to provide cross sections of the empty basin floor. A digital automatic level was used to confirm elevation readings made with the total station to ensure that the basin floor and scan data were level.

3.4.4 Results

Further investigation revealed that the Southeast Benchmark elevation on record was approximately 75mm higher than observed with a survey-grade level, which alone accounts for approximately 0.11 degrees of the observed error. Attempts to explain the cause of such a large error would be

speculative, although historical data indicate that the presence of this error resulted in the rotation and corruption of the wave basin's control network over several years as it propagated through subsequent surveys by the professional firm and lab technicians.

The use of the scanner's built-in inclination sensor in this study provided a check on the control coordinates and quickly alerted operators to the problem, demonstrating the value of using the inclination sensor as a quality control tool. Additionally, once new control coordinates had been determined for the wave basin, Set 2 was then successfully registered to the local coordinate system using the same level-constrained ICP software alignment as before, saving operators the field time that would have been necessary to scan tiepoints for every scan position. With the new control coordinates, the alignment of Sets 1 and 2 were consistent, as shown in Figure 9B and D. The quality of the inclination sensor-derived data was also confirmed using cross sections measured using a digital level and total station.

3.5 CONCLUSION

There is a tacit assumption among TLS users that inclination sensors in laser scanners behave similarly to their traditional operation in total stations. For scanners that pause rotation during scanning, this assumption appears to be sound as long as the scanner pauses for a sufficient amount of time. It has

been shown that TLS inclination sensor results are influenced by scanner motion during scanning and therefore must be treated differently than those of total stations, particularly for rapid scanners.

While some of the inertial error can be reduced by measuring inclination data during scans in both a clockwise and counter-clockwise direction, some random error will still exist, possibly due to the physical mechanics of measuring during laser scanning. This inertial error also varies with the rotating scanner head's position at the time of measurement; therefore, scans used to measure precise inclination data should encompass a full 360° horizontal scan window.

Even on those occasions when a scanner is leveled as accurately as possible, a small amount of error will always exist. Unless inclination data is recorded for each setup, it is difficult, even impossible, to determine by inspection whether a point cloud is actually leveled, particularly since the scan setup is generally close to level. A properly leveled point cloud is significantly easier to work with and transfer between software packages than one tilted in space.

Leveling tests were conducted in a controlled lab setting with the inclination sensor enabled. These tests investigated whether scanner rotation speed correlated with inclination data quality and then developed a recommended minimum 360° scan duration—a "stability threshold"—that ensured reliable

inclination data. For the scanner used in this study, a minimum recommended scan time of 100 seconds (2 minutes to be conservative) balances the need for efficient field work with reliable inclination sensor data. Note that the same results were achieved regardless of whether or not the instrument was precisely leveled. These tests verified both the accuracy and precision of the laser scanner's inclination sensor, provided that the scanner rotates slowly enough for measurements taken during scanning.

It is recommended that those who rely on inclination data for control should perform a similar stability threshold evaluation for their scanner to ensure that they achieve reliable results. Alternatively, inclination data derived from a method similar to the continuous measurement method shown in Table 3—where inclination measurements are averaged from 360° rotations clockwise and counter-clockwise—has also shown itself to be reliable.

The case study presented herein has demonstrated that inclination sensors can be a reliable and inexpensive means to verify control coordinates and scan data. The additional redundancy provided by the inclination sensors and using more than the minimum control prevented propagation of the leveling errors encountered in this case study. It must be emphasized that while laser scanning may be considered different from traditional surveying, it must still

follow the same principles of redundancy and systematic procedures to avoid major blunders.

3.6 ACKNOWLEDGEMENTS

Partial funding for this research was provided through OTREC under project 2011-398. The authors would like to thank Leica Geosystems and David Evans & Associates for their generous provision of training, equipment, and software to Oregon State University. Maptek Pty donated licenses and support for Maptek I-Site Studio. Riegl Laser Measurement Systems provided their RiVLib API and technical support for the Riegl VZ-400. Shawn Butcher (OSU CCE doctoral student) and Tim Maddux (HWRL) assisted with data collection and background information. Finally, Gene Roe of lidarnews.com and administrators of laserscanning.uk helped distribute the inclination sensor survey. We appreciate those who participated in the survey and shared their unique insights.

4 FIELD APPLICATIONS OF TLS REFERENCE FRAME TRANSFORMATIONS

Surveyors and geomatics professionals provide a valuable service as measurement and spatial data modeling experts. Several collaborative efforts with other members of the Oregon State University research community were undertaken for training, database enrichment, and field testing. Projects related to research conducted at the O. H. Hinsdale Wave Research Laboratory (HWRL) on the Oregon State University campus will be highlighted in this section.

4.1 THE HWRL TSUNAMI WAVE BASIN COORDINATE SYSTEM

The need for a new local coordinate system in the HWRL Tsunami Wave Basin (TWB) was first introduced in Section 3.4. The detailed analysis behind the development of that coordinate system was outside the scope of the manuscript presented in Chapter 3. This section will present discussion of the methodology and insights it provides on laser scanning technology.

The new coordinate system definition required four conditions (see Figure 10) to simplify use in scientific research:

1. The origin (0, 0, 0) must be located at the base and center of the wavemaker face as it rested on June 23, 2010.
2. The average of the floor defines the vertical datum ($Z = 0$).

3. The wavemaker face defines the *Y* axis such that *X* = 0 along its length.
4. The coordinate system must be right-handed.

Note that north in the global sense follows the –*Y* direction in the local coordinate system. While this may seem counterintuitive, such an orientation makes experimental results from the TWB consistent with the West Coast of the United States, with waves approaching from the –*X* direction, or "west."

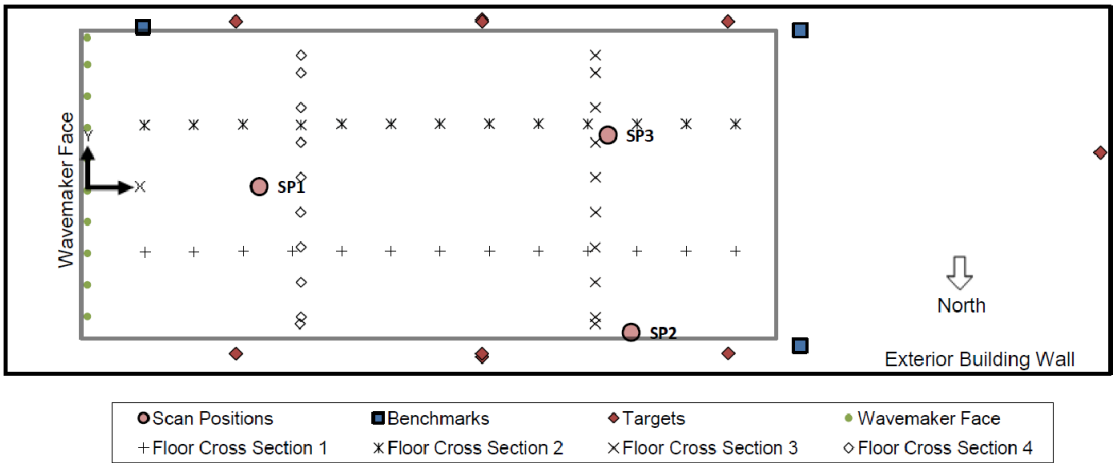

Figure 10: Plot of total station points recorded around the TWB in July, 2010. Note that the wavemaker face is on the left in this figure, with positive *X* pointing right and positive *Y* pointing up.

4.1.1 Data Collection

On July 13, 2010, high-resolution 360° scans of the empty and mostly dry TWB were collected from three leveled scan positions, above the stability threshold. Five targets (Figure 7) distributed around the TWB on supporting columns were scanned at fine resolution from each scan position. Coordinates obtained from a total station were collected in an arbitrary coordinate system

for every target and benchmark, across the wavemaker face, and in four cross sections on the floor (Figure 10).

Following collection in the field, the point cloud from each scan setup was leveled programmatically using its inclination values. Total station coordinate data was processed and treated as control data due to its very high precision. Digital leveling data was also collected, where possible, to verify elevations collected with the total station. In all cases, the total station and digital level elevation values agreed within 1 millimeter. Finally, target tiepoints were extracted from the fine-resolution scans for each setup in preparation for tiepoint registration.

4.1.2 Development of the New TWB Control Coordinate System

The six-step development of the new HWRL TWB control coordinate system is detailed in Figure 11. Between each step, the scans were aligned using tiepoint registration—a least squares adjustment technique that matches the scan-based tiepoints to the updated total station control points. In summary, the key steps are:

1. Shift to an arbitrary, workable coordinate system.
2. Translate in the Z direction such that, on average, Z = 0 on the empty floor.

3. Rotate around the Z axis such that the wavemaker face is parallel to the Y axis and the X axis points into the wave basin.
4. Translate in the XY plane such that the new origin is in the center of the wavemaker face.
5. Verify proper alignment between scans using the new control.
6. Verify agreement between scan and total station data. Repeat as necessary.

The end result of this work was a new coordinate system that has been used without any problems following its development. It is worthwhile to note that the TLS data collection required significantly less field time than the total station and provided much more intuitive models with denser data. Furthermore, the coordinate system could have been developed using only one or two scan setups. Three scan positions were used to provide redundancy to evaluate the quality of the scan data.

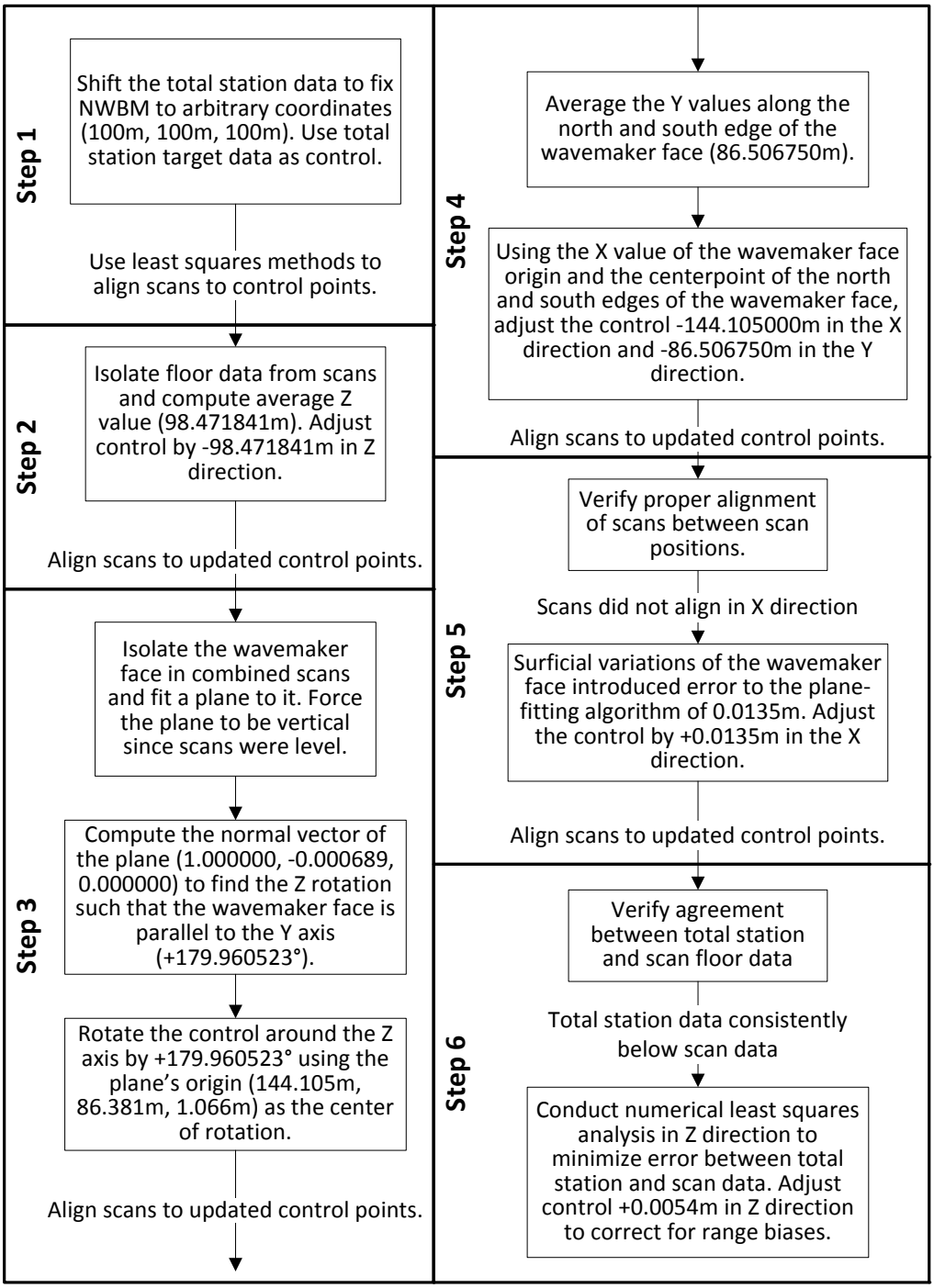

Figure 11: Flowchart detailing the steps toward developing the new HWRL TWB control coordinate system.

4.1.3 Additional Considerations

The wavemaker face shows significant variability (±0.05 meters) in the *X* direction due to its construction as a series of independently-controlled panels and warping of the panels themselves (Figure 12). While this variation went essentially undetected in the ten total station data points, it was clear upon examination of the LiDAR data, demonstrating the value of TLS for rapidly recording complex geometric shapes. However, the high-precision total station data did provide a reliable check that enabled the correction of the 1.35 centimeter error observed in Step 5. The source of this error appears to be saturation effects due to scan position 1 being too close to the wavemaker face, a highly reflective surface (Vosselman and Maas 2010).

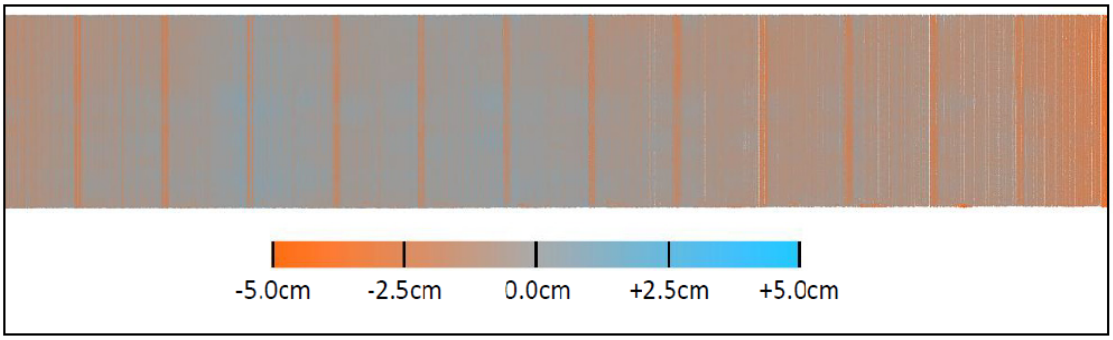

Figure 12: A portion of the wavemaker face, colored according to distance from the plane computed in Step 3. Negative (orange) values indicate that the point was closer to the scan position than the plane.

The 5 millimeter discrepancy between the TLS data and total station data observed in Step 6 led to an investigation to uncover its cause. The TWB floor as scanned from three different positions is shown in Figure 13.

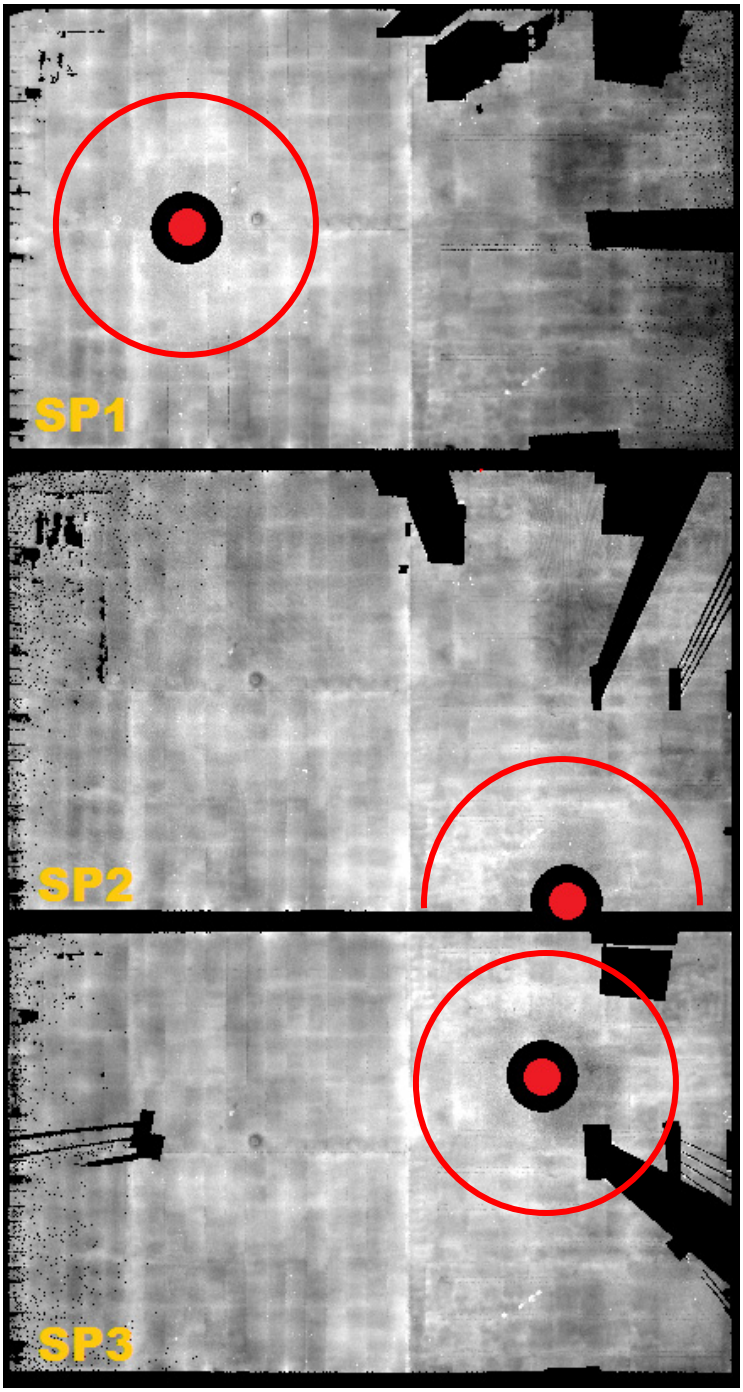

Figure 13: TLS data of the TWB floor from three different scan positions, colored according to elevation. White points are at Z ≥ 0.01m. Note the concentration of these points close to the scanner that are not observed in the other scan positions.

The white patch surrounding a scan position does not appear in the corresponding area in the other two scans. This suggests that points close to the scanner have a slight (approximately 5 mm) bias that makes them appear closer than they otherwise would. As the scanner used in this study was calibrated as a long-range (>100 meters) scanner, this explanation for the 5.4 millimeter discrepancy in Step 6 of the previous section seems plausible.

This becomes especially clear while comparing the cross sections in Figure 14 (east-west) and Figure 15 (north-south) to the relative scan position locations shown in Figure 13. Prior to the 5.4 millimeter correction in Step 6, the total station data (orange circles) were consistently below the scan data, even after accounting for the noticeable variations in the TWB floor itself. The numerical least squares adjustment corrected this error to shift the control up such that the total station data would, on average, align with the scan data.

Using either a coordinate system such as the one developed in this section or by implementing the leveling methods detailed in the Chapter 3, laser scan registration can be done rapidly and easily with minimal user input.

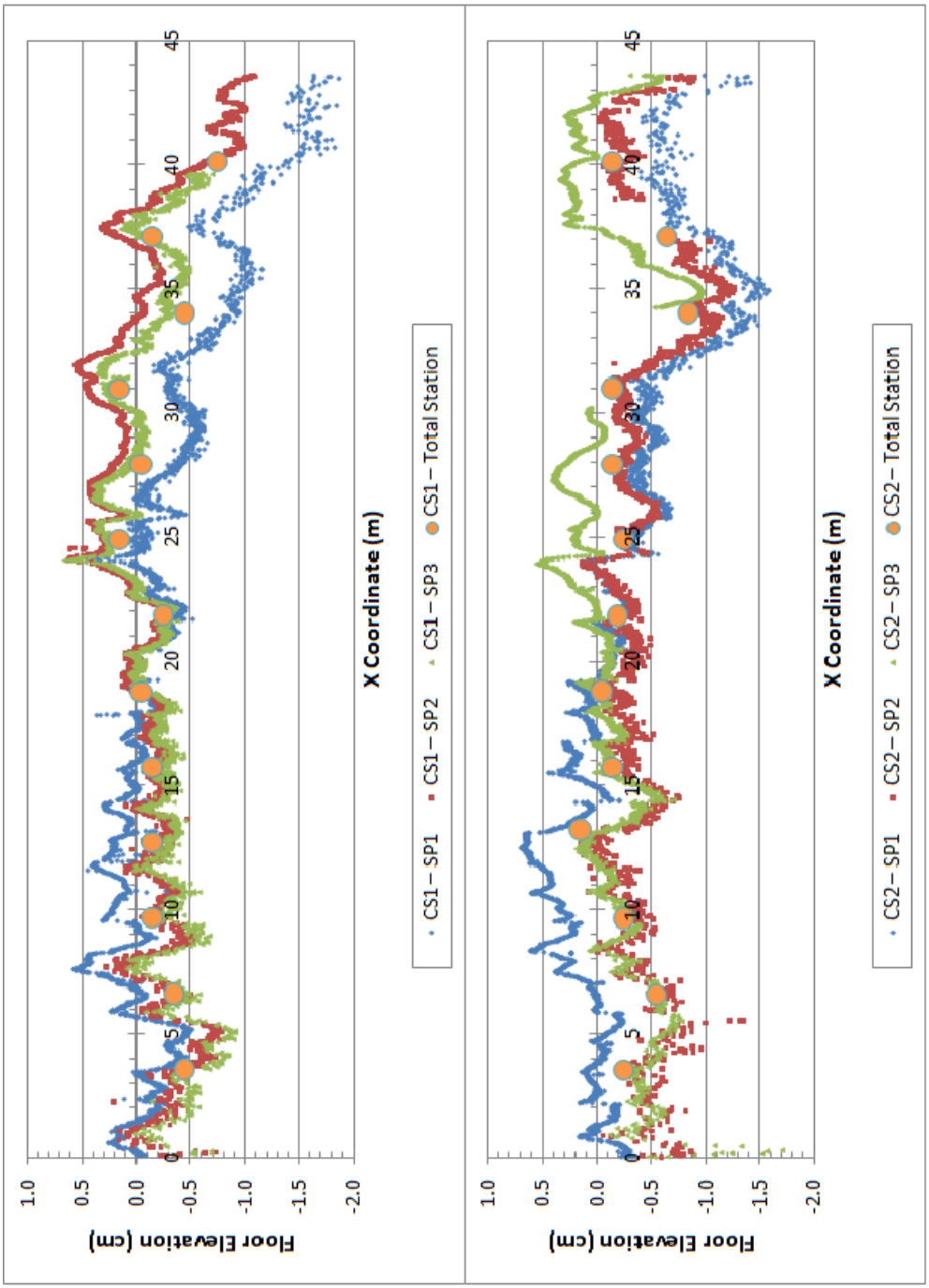

Figure 14: East-west cross sections (CS) of the TWB floor, separated by scan position (SP).

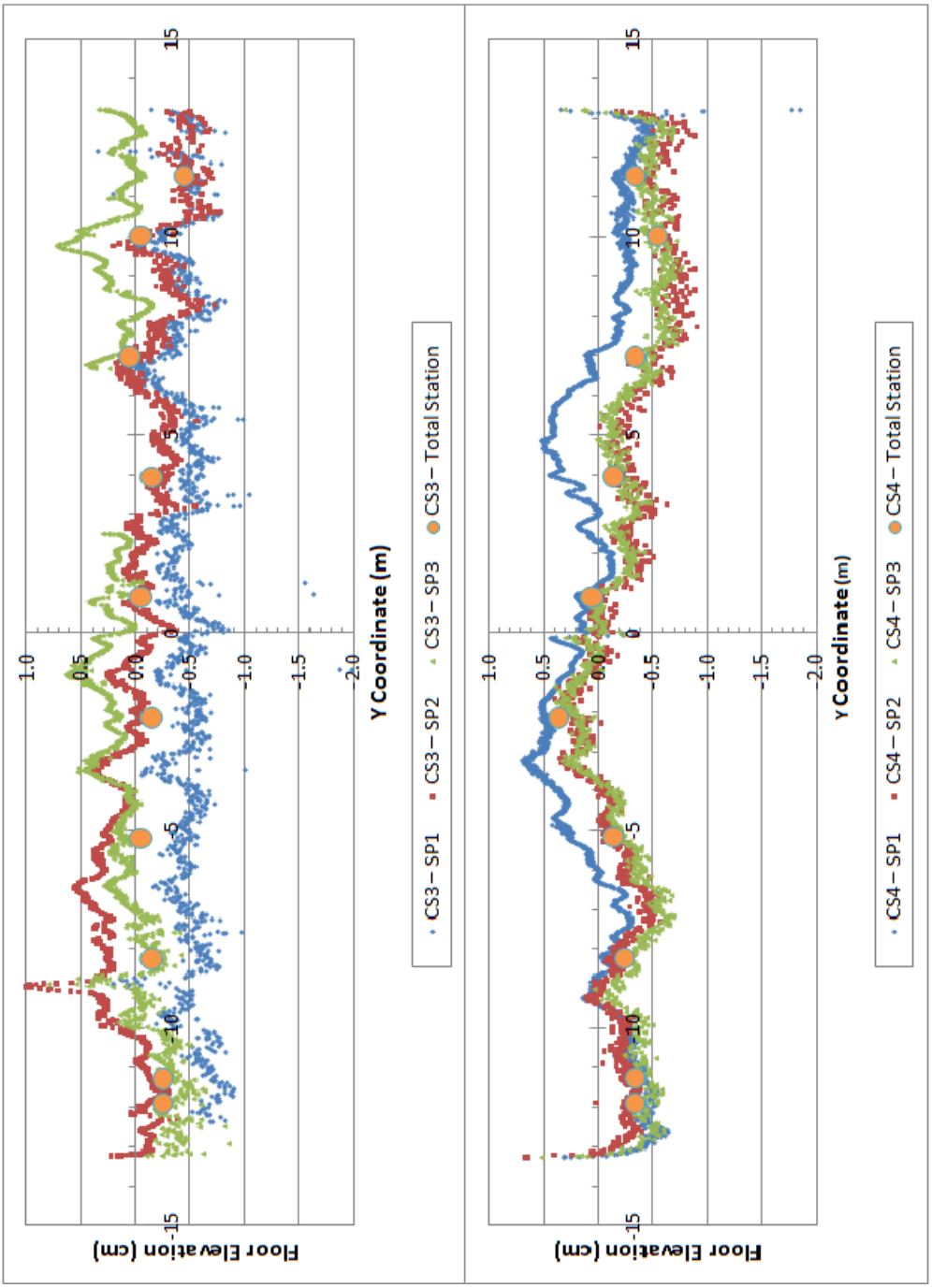

Figure 15: North-south cross sections (CS) of the TWB floor, separated by scan position (SP).

4.2 REAL-TIME CHANGE DETECTION

Because of its flexibility, speed, and efficiency, terrestrial laser scanning has shown promise as a valuable tool to efficiently detect and measure change in real time. Figure 16 shows an example of post-processed change detection applied to a project in the HWRL. Similarly, Figure 17 shows a gusset plate scanned during load testing with change detection relative to a planar surface. Color coding similar to what is seen in either figure can be implemented in real time for rapid user feedback.

By combining change detection algorithms with the surface matching, azimuth adjustment technique developed by Olsen, et al. (2009, 2011), future researchers will be able to detect change using a mobile computer in the field, rather than the traditional workflow of returning to the office to process data for change analysis. That “augmented reality” data could be used to immediately determine areas that require scanning at higher resolutions, reducing unnecessary data collection field time and eliminating the need to return to the site due to poor coverage. A lightweight, Qt-based scanner interface was developed through this research in order to enable automatic collection, registration, adjustment, and analysis of scan data from a Riegl VZ-400. See Appendix C for instructions in its use. This program implements the inclination sensor recommendations developed in the previous chapters.

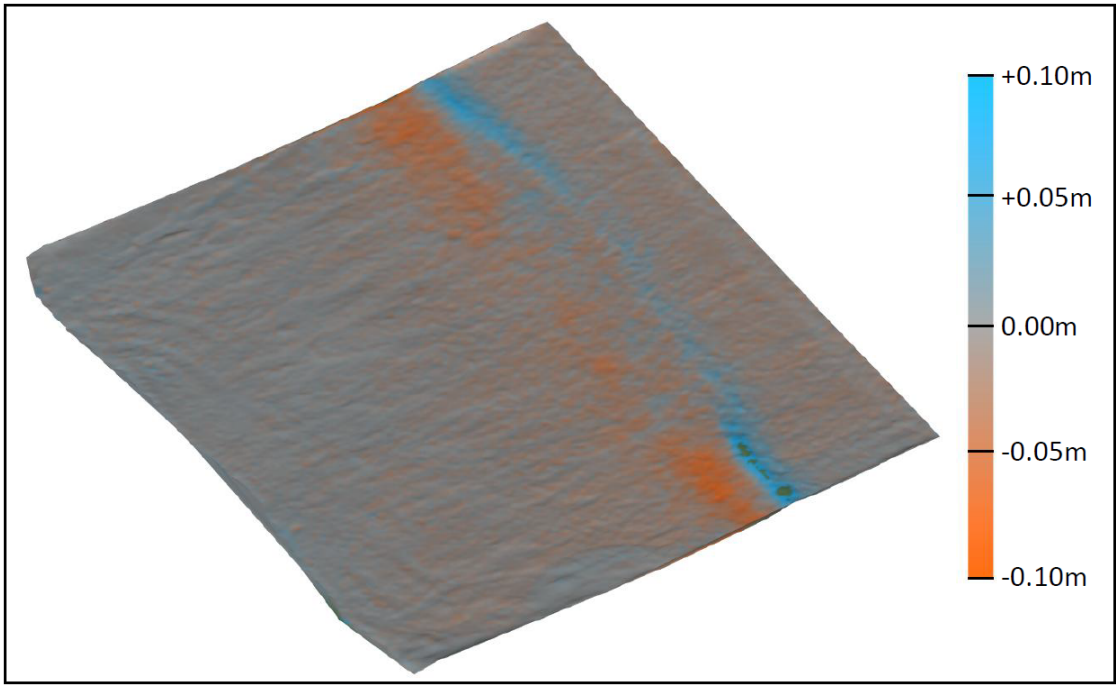

Figure 16: Point cloud data set of a model beach at the HWRL, after wave inundation. Blue represents accretion and orange represents erosion.

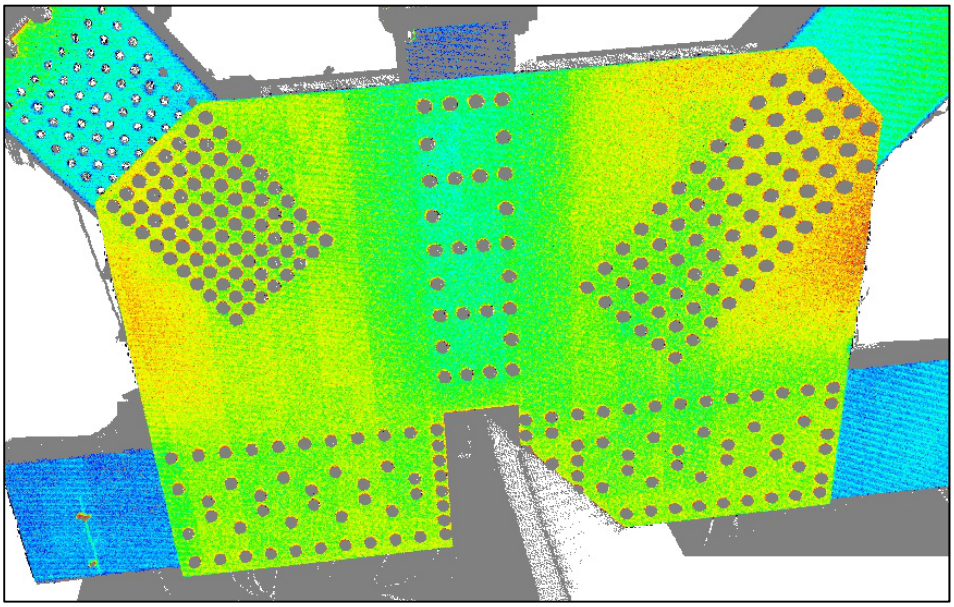

Figure 17: A gusset plate scanned before and after load testing colored according to deviations from a plane. Red indicates large displacements.

5 OVERALL CONCLUSION

The research presented herein revealed current limitations of terrestrial laser scanning technology relevant to reference frame transformations and adjustments and recommended solutions to enable broader use.

5.1 COORDINATE TRANSFORMATION AND ADJUSTMENT

Least squares methods applied to a seven-parameter, three-dimensional similarity adjustment traditionally require an iterative, nonlinear solution. This process can be computationally intensive, and increasingly so as the data set increases in size. This can be an issue when working with TLS data, as millions of points can be collected in a single scan. An alternative to the traditional least squares solution presented in Han (2010b) known as the NonIterative Solution to Linear Transformations (or NISLT) technique attempts to overcome this issue.

While the NISLT technique appears to be both fast and efficient, the rotation matrix estimated by NISLT does not possess the properties of a true rotation matrix. Therefore, the derived rotation angles and the root mean square error from the NISLT adjustment may be unreliable. It has been demonstrated numerically that a linear least squares solution or NISLT solution can be constrained using the properties of a rotation matrix in order to overcome this limitation, but an analytical solution to implement this noniteratively remains to

be discovered. Future research should investigate quaternion rotations as a possible solution. Additionally, the NISLT technique in its current form appears to be more sensitive to outliers than traditional least squares methods, but more research using poor-quality data is required to confirm this.

5.2 INCLINATION SENSORS

Inclination sensors in modern terrestrial laser scanners have been demonstrated to be useful and reliable when used properly. For example, inclination sensor data can be a valuable quality check on control data used for point cloud registration. However, it has been shown herein that inclination sensor data quality can degrade while scanning at high scanner head rotation speeds.

This inertial-based degradation can be reduced, cancelled, or avoided through proper field techniques and scan planning. A scan duration longer than a “stability threshold” ensures quality inclination data. Alternatively, measuring inclination data in both clockwise and counter-clockwise directions separately from the actual scanning has also been shown to effectively eliminate inertial effects. In all cases, a full 360° rotation is recommended to remove systematic bias.

5.3 TLS Reference Frame Transformations in the Field

A case study has been presented in which total station and TLS data were used to successfully develop a new coordinate system with a geometrically controlled definition. The TLS data collection was significantly faster and provided a more robust solution for the geometric objects, although the inclusion of some total station data also provided reliable checks against the TLS data when discrepancies were discovered. Further study is required to determine the cause of these discrepancies.

TLS data collection also lends itself well to automation, making it attractive for real-time change detection applications. A lightweight scanner interface has been developed to facilitate this automation through integration with other analysis tools. Research in this area is ongoing at Oregon State University.

WORKS CITED

Agosto, Eros, Andrea Ajmar, Piero Boccardo, Fabio Giulio Tonolo, and Andrea Lingua. "Crime Scene Reconstruction Using a Fully Geomatic Approach." *Sensors* 8, no. 10 (2008): 6280-6302.

Anderson, James M, and Edward M Mikhail. *Surveying: Theory and Practice.* 7th Edition. WCB/McGraw-Hill, 1998.

Barber, David, Jon Mills, and Sarah Smith-Voysey. "Geometric validation of a ground-based mobile laser scanning system." *ISPRS Journal of Photogrammetry and Remote Sensing* 63, no. 1 (January 2008): 128-141.

Bernardini, Fausto, Holly Rushmeier, Ioana M Martin, Joshua Mittleman, and Gabriel Taubin. "Building a Digital Model of Michelangelo's Florentine Pietá." *IEEE Computer Graphics and Applications* 22, no. 1 (Jan./Feb. 2002): 59-67.

Besl, P. J., and N. D. McKay. "A method for registration of 3D shapes." *IEEE PAMI* 14, no. 2 (1992): 239-256.

Boehler, W, M Bordas Vicent, and A Marbs. "Investigating Laser Scanner Accuracy (Updated Online 2004)." *i3mainz.* April 2004. http://scanning.fh-mainz.de/scannertest/results200404.pdf (accessed November 15, 2010).

Cuartero, Aurora, Julia Armesto, Pablo G Rodriguez, and Pedro Arias. "Error Analysis of Terrestrial Laser Scanning Data by Means of Spherical Statistics and 3D Graphs." *Sensors* (MDPI), November 2010: 10128-10145.

Dunning, S.A., N.J. Rosser, and C.I. Massey. "The integration of terrestrial laser scanning and numerical modelling in landslide investigations." *Quarterly Journal of Engineering Geology and Hydrogeology* 43 (2010): 233-247.

FARO Technologies Inc. *FARO LS 880 Techsheet (English).* January 21, 2009. http://www.faro.com (accessed November 30, 2010).

Ghilani, Charles D. *Adjustment Computations: Spatial Data Analysis.* 5. Hoboken, NJ: John Wiley & Sons, Inc., 2010.

Han, Jen-Yu. "A Noniterative Approach for the Quick Alignment of Multistation Unregistered LiDAR Point Clouds." *IEEE Geoscience and Remote Sensing Letters* 7, no. 4 (October 2010): 727-730.

Han, Jen-Yu. "Noniterative Approach for Solving the Indirect Problems of Linear Reference Frame Transformations." *ASCE Journal of Surveying Engineering* 136, no. 4 (November 2010): 150-156.

Han, Jen-Yu, Jenny Guo, and Jun-Yun Chou. "A Direct Determination of the Orientation Parameters in the Collinearity Equations." *IEEE Geoscience and Remote Sensing Letters* 8, no. 2 (March 2011): 313-316.

JADA Productions. "Laser Scanner Hardware Survey." *Point of Beginning.* Edited by Christine L. Grahl. 2010. http://laser.jadaproductions.net/hardware/default.php (accessed November 15, 2010).

Jekeli, Christopher. *Inertial Navigation Systems with Geodetic Applications.* Berlin: de Gruyter, 2001.

Leica Geosystems AG. *Leica ScanStation C10 Technical Datasheet (English US).* 2011. http://hds.leica-geosystems.com/en/Leica-ScanStation-C10_79411.htm (accessed February 24, 2011).

Lichti, Derek D. "Error modelling, calibration and analysis of an AM-CW terrestrial laser scanner system." *ISPRS Journal of Photogrammetry & Remote Sensing* 61 (2007): 307-324.

Lichti, Derek D, and Maria Gabriele Licht. "Experiences with Terrestrial Laser Scanner Modelling and Accuracy Assessment." *International Archives of Photogrammetry and Remote Sensing* 36, no. Part 5 (September 2006): 155-160.

Lichti, Derek D, Stuart J Gordon, and Taravudh Tipdecho. "Error Models and Propagation in Directly Georeferenced Terrestrial Laser Scanner Networks."

Journal of Surveying Engineering (ASCE) 131, no. 4 (November 2005): 135-142.

Mechelke, Klaus, Thomas P. Kersten, and Maren Lindstaedt. "Comparative Investigations into the Accuracy Behaviour of the New Generation of Terrestrial Laser Scanning Systems." Edited by A. Gruen and H. Kahmen. *Optical 3-D Measurement Techniques VIII.* Zurich, 2007. 319-327.

Olsen, Michael J, Elizabeth Johnstone, Falko Kuester, Neal Driscoll, and Scott A. Ashford. "New automated point-cloud alignment for ground-based light detection and ranging data of long coastal sections." *Journal of Surveying Engineering* (ASCE) 137, no. 1 (February 2011): 14-25.

Olsen, Michael J, Elizabeth Johnstone, Neal Driscoll, Scott A Ashford, and Falko Kuester. "Terrestrial Laser Scanning of Extended Cliff Sections in Dynamic Environments: Parameter Analysis." *Journal of Surveying Engineering* (ASCE) 134, no. 4 (November 2009): 161-169.

Ravani, Bahram, Jagannath Hiremagalur, Kin S. Yen, Kevin Akin, Triet Bui, and Ty A. Lasky. *Creating Standards and Specifications for the Use of Laser Scanning in Caltrans Projects.* AHMCT Final Report, California AHMCT Program, University of California at Davis, 2007.

RIEGL LMS GmbH. *RiSCAN PRO v1.5.7.* May 18, 2011.

Salvi, Joaquim, Carles Matabosch, David Fofi, and Josep Forest. "A review of recent range image registration methods." *Image and Vision Computing* 25, no. 5 (May 2007): 578-596.

Skaloud, Jan, Philipp Schaer, Yannick Stebler, and Phillip Tomé. "Real-time registration of airborne laser data with sub-decimeter accuracy." *ISPRS Journal of Photogrammetry and Remote Sensing* 65, no. 2 (March 2010): 208-217.

Son, Seokbae, Hyunpung Park, and Kwan H Lee. "Automated laser scanning system for reverse engineering and inspection." *International Journal of Machine Tools and Manufacture* 42, no. 8 (June 2002): 889-897.

Vosselman, George, and Hans-Gerd Maas. *Airborne and Terrestrial Laser Scanning.* North American. Caithness, Scotland: Whittles Publishing, 2010.

Vuylsteker, Pascal. *Computer Graphics : 3D Transformation : 14 / 19 : Properties of the Rotation Matrix.* April 20, 2004. http://escience.anu.edu.au/lecture/cg/Transformation/rotationMatrixProp.en.html (accessed May 18, 2011).

Wehr, Aloysius, and Uwe Lohr. "Airborne laser scanning—an introduction and overview." *ISPRS Journal of Photogrammetry & Remote Sensing* 54 (1999): 68-82.

Wynne, Randolph H. "Lidar Remote Sensing of Forest Resources at the Scale of Management." *Photogrammetric Engineering & Remote Sensing* (ASPRS), December 2006: 1310-1314.

APPENDICES

APPENDIX A – LEAST SQUARES ANALYSIS PROGRAM NOTES

Least Squares User Manual

5/19/2011
By Evon Silvia, Graduate Research Assistant, School of Civil and Construction Engineering
evon.silvia@gmail.com

Introduction

The Least Squares program is a simple Qt interface that receives a set of matching point pairs and performs a traditional, un-weighted, nonlinear least squares adjustment and reports the results. The "adjustnonlinear" C++ class was written to be easily integrated into other programs if desired.

Application of the resultant transformation to additional points must be done manually by the user.

Data preparation

Input files must be comma-delimited ASCII files, with X,Y,Z coordinates followed by a newline character on every line. Comment lines must begin with a "#" character. The control and measured data must have the same number of points, with corresponding points following the identical order in both input files. The file must also end with a newline character (a blank line).

General procedure

For details regarding the nonlinear least squares solution see Evon Silvia's thesis "Overcoming the Level Bubble: Dynamic Terrestrial Laser Scanning Reference Frame Transformations," 2011, Oregon State University or the textbook "Adjustment Computations: Spatial Data Analysis" by Charles Ghilani (5th Edition, 2010).

Upon opening, the program immediately requests the user to select a CSV or TXT file with control data to remain fixed, and then again for measured data to be adjusted. These files must have the same number of points.

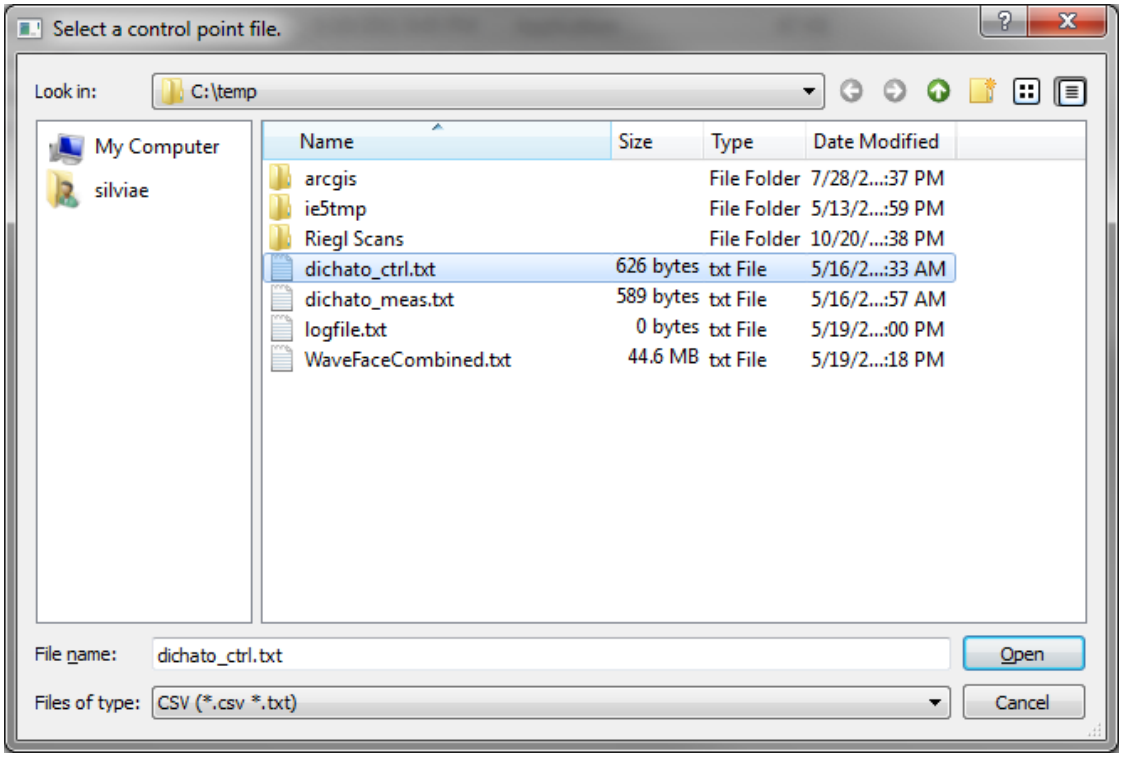

Figure A1: The control point file loading screen.

If loading succeeded, then the user may start the adjustment by clicking [Start].

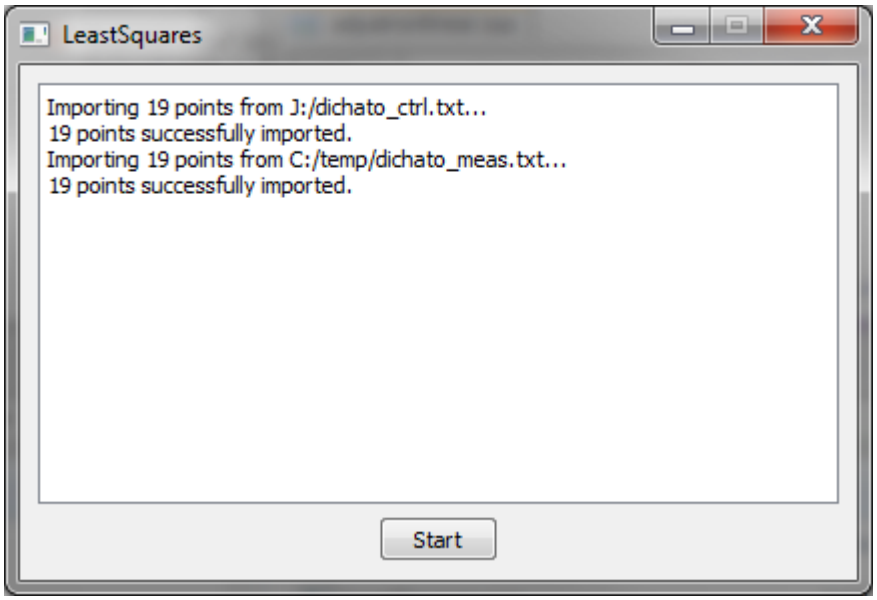

Figure A2: Verify that the correct number of points loaded from each file prior to clicking [Start].

The program currently seeds the iterative process with rotations and translations of 0 and a scale factor of 1. This may be an issue for some data sets that will be unable to converge without good initial values.

The program will iterate up to 200 times or until the new RMS has changed less than 0.000001 from the previous iteration, whichever comes first. The rotation angles are forced to be between 0 and 2π after each iteration to prevent value inflation.

For each iteration, a Jacobian matrix populated by the first-order Taylor series polynomials of

$$\begin{bmatrix} X' \\ Y' \\ Z' \end{bmatrix} = S \begin{bmatrix} r_{11} & r_{12} & r_{13} \\ r_{21} & r_{22} & r_{23} \\ r_{31} & r_{32} & r_{33} \end{bmatrix} \begin{bmatrix} x \\ y \\ z \end{bmatrix} + \begin{bmatrix} T_x{}' \\ T_y{}' \\ T_z{}' \end{bmatrix}$$

is calculated, where

$$\begin{aligned} r_{11} &= \cos\theta_2 \cos\theta_3 \\ r_{12} &= \cos\theta_1 \sin\theta_3 + \sin\theta_1 \sin\theta_2 \cos\theta_3 \\ r_{13} &= \sin\theta_1 \sin\theta_3 - \cos\theta_1 \sin\theta_2 \cos\theta_3 \\ r_{21} &= -\cos\theta_2 \sin\theta_3 \\ r_{22} &= \cos\theta_1 \cos\theta_3 - \sin\theta_1 \sin\theta_2 \sin\theta_3 \\ r_{23} &= \sin\theta_1 \cos\theta_3 + \cos\theta_1 \sin\theta_2 \sin\theta_3 \\ r_{31} &= \sin\theta_2 \\ r_{32} &= -\sin\theta_1 \cos\theta_2 \\ r_{33} &= \cos\theta_1 \cos\theta_2 \end{aligned}$$

The K matrix as defined by Ghilani is then computed based on the results of the previous iteration (or the initial guess for the first iteration), and the corrections for the current iteration are computed by

$$\boldsymbol{e} = \left(\boldsymbol{J^T W J}\right)^{-1} \boldsymbol{J^T W K}$$

The inverse is computed using the C++ code provided by Ghilani (2010) in Table B.1. More efficient methods exist, but this one works and is easy to implement. Transformation parameters are then updated and the measured points are re-transformed for the next iteration.

Once the exit conditions are met, the results are printed to a text box.

Interpreting results

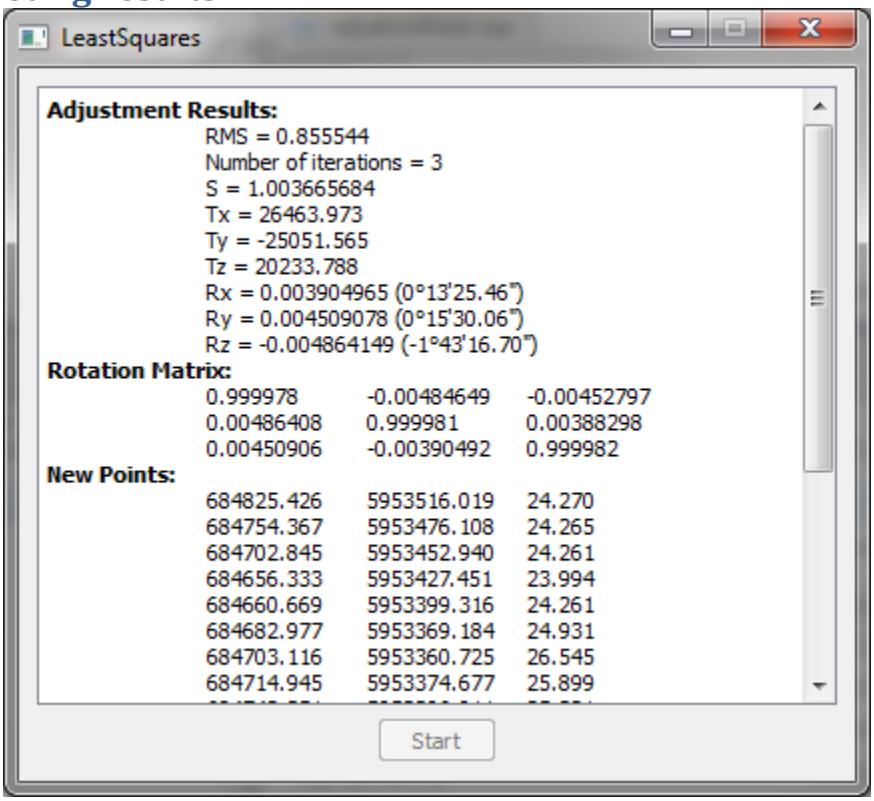

Figure A3: Adjustment results will be shown on a screen similar to this one. Rotation angles are in radians and Degrees-Minutes-Seconds. Copy and paste this output to a blank text file if you want to save it.

The results printed are fairly straightforward and can be copied to your favorite text editor or spreadsheet to be saved.

- RMS is a report of the Root Mean Square error, which is a measure of the quality of the match between the input data sets.
- Usually no more than 10 iterations are required to find a match. If there are more, there may be issues with the adjustment.
- S is the scale parameter.
- Tx,Ty,Tz is the translation vector.
- Rx,Ry,Rz are the rotation angles in radians or DMS.
- The rotation matrix is computed from Rx,Ry,Rz (see equations in Silvia (2011)).
- The new points are the transformed points from the measured point file after the final iteration.

APPENDIX B – NISLT MATLAB SCRIPT NOTES

NISLT Matlab User Manual

5/19/2011
By Evon Silvia, Graduate Research Assistant, School of Civil and Construction Engineering
evon.silvia@gmail.com

Introduction

The `adjustHan(ctrlPath,measPath)` MATLAB script performs an optimized version of the similarity NISLT adjustment as developed and presented by Jen-Yu Han in

> Han, Jen-Yu. "Noniterative Approach for Solving the Indirect Problems of Linear Reference Frame Transformations." ASCE Journal of Surveying Engineering 136, no. 4 (November 2010): 150-156.

The syntax for the command simply requires two windows-style file paths to two comma-delimited ASCII files, one for control data and one for measured data. A call to this function will look something like this:

```
adjustHan('J:\mon_ctrl.txt','J:\mon_meas.txt');
```

The function will match the points in order (the first point with the first point, the second with the second, etc), so ensure that they are sorted to match. It uses the Matlab `csvread(filename)` function to import the points, so follow the formatting rules for that function.

Output

The function will output a series of text that will look something like the following:

```
>> adjustHan('c:\temp\5pt-ctrl.txt','c:\temp\5pt-meas.txt');
Raw Rotation Matrix (R-hat):
         0.407777391022836        -0.914294786828213         0.0562338900691944
         0.913640618333182         0.407352352919333         0.0297736416791388
      0.000212293795449796    -8.42174476038914e-005           0.99794047648357

Recomputed Rotation Matrix (R-calc):
         0.407569252666347        -0.913174286505208     -0.000163544184471777
         0.913174276498378         0.407569276741785     -0.000159367005069884
       0.00021218543612765    -8.43912511745261e-005          0.999999973927728

Derived rotation around x (alpha) (rad,deg):
     8.43912531744563e-005       0.00483526263471635

Derived rotation around y (beta) (rad,deg):
      0.000212185437719842         0.012157330055483

Derived rotation around z (gamma) (rad,deg):
         -1.15100570648747         -65.9477691772056

Translation vector:
          34788.213974199
          26069.4690880224
```

```
          73.8516663028582

Updated translation vector:
          34788.213499084
          26069.4773608414
          73.8513886331855

Scale:
         0.999663999733704

Transformed points (R-hat):
             34758.4534357          26096.9804999565          74.5920597106532
          34775.3889262245          26105.9926083108          74.0473863268673
          34795.3742079115          26087.4272506351          73.8420325614988
          34819.1617829325          26061.7720804411          73.0923313997251
          34775.5326472315          26077.0495606564          74.3751900012557

or... (R-calc):
          34758.4513983188          26096.9688260255          74.5933029359046
          34775.4015314734           26105.987775405          74.0474972076757
          34795.3713596344           26087.427098077          73.8417244584684
          34819.1680899039          26061.7938219339          73.0904835942779
          34775.5186206694          26077.0444785586          74.3759918036734

RSME R-hat, R-Calc (new T):
       0.00573323275059479
        0.0157220817750252
```

The pseudo-rotation matrix R-hat ($\widehat{\boldsymbol{R}}$), Scale ($\hat{s}$), the Translation vector ($\hat{\boldsymbol{t}}'$), and the rotation angles (r_x, r_y, r_z) are the same as defined in Han (2010) for the similarity model. However, it was observed that $\widehat{\boldsymbol{R}}$ is not a true rotation matrix, and as such the rotation matrix computed using the rotation angles (R-calc) will not be the same. That calculated rotation matrix, the new translation vector derived from it, and the new set of transformed coordinates are also provided in addition to the typical results from the NISLT technique.

A Root Mean Square Error is also calculated using the results of both techniques.

Optimizations

One simple optimization was made to the original NISLT method to reduce memory usage and computation time. Rather than computing scale and the ΔX terms over the range of $i \neq j$, we computed for $j > i$ where i increments from 1 to n-1, and j increments from i to n, where n is the number of point pairs. This removes redundancy introduced by computing the same distance (ij and ji) twice.

APPENDIX C – SCANNER INTERFACE PROGRAM NOTES

DriveVZ400 User Manual

5/19/2011
By Evon Silvia, Graduate Research Assistant, School of Civil and Construction Engineering
evon.silvia@gmail.com

Introduction

The DriveVZ400 tool is a convenient, lightweight scan collection interface that can run by itself or within other programs. It cannot process data—it can only record. It can be used on any windows-based device with networking capabilities and all of the information needed to record a scan is conveniently displayed on one screen. It also supports automatic or command-line operation.

Several other viable options exist to operate the RIEGL VZ-400 scanner.

- On-board interface. This is the most straightforward manner, but the menu structure can be counter-intuitive and inconvenient. Simple operations like entering a project name require pressing buttons repeatedly. Every time you press a button the scanner's setup has been disturbed a small amount, which can be a problem in high-precision work.
- RiSCAN PRO. Every laptop and computer in the lab has RiSCAN PRO installed, which can run the scanner either wirelessly or through an Ethernet connection. This program can open, display, edit, and process the raw data produced by the scanner. It can also conveniently record new scans based on the previous scans.
- Telnet. The scanner can be connected to using telnet, a command-line communication protocol. This sends raw commands that the scanner interprets. A list of these commands and their use is in the scanner's manual. RiSCAN PRO and DriveVZ400 both use these commands in a manner invisible to the user.

Connecting to the scanner

Open the executable either by double-clicking it or running it from the command-line—see the next section for instructions using the script codes. The interface should appear.

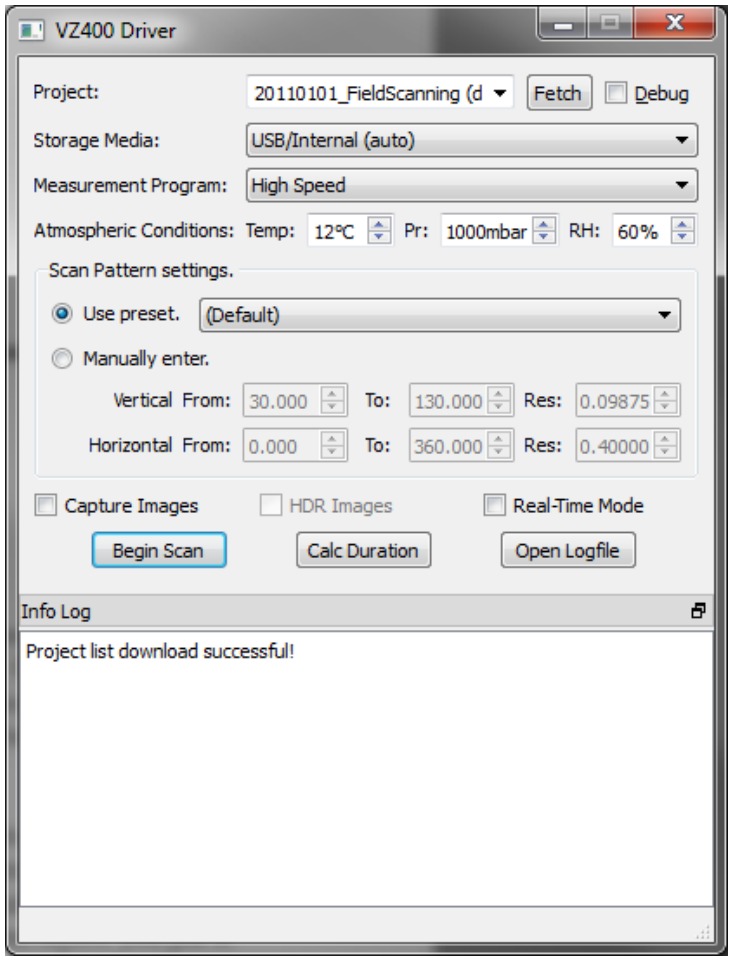

Figure C1: The DriveVZ400 main screen.

Connecting to the scanner is fairly straightforward and can be done in one of two ways:

- Wireless. Once it has powered up the scanner becomes a wireless hotspot just like a normal router. The network name is the same as its serial number (S########) and uses WEP encoding. Check with the lab manager to get the network password if you don't have it. This connection can be a little slow when downloading raw data files.
- Ethernet (wired). The VZ400 has two Ethernet ports, one on the base requiring a special adapter (100MBit) and one on the scanner head itself (1GBit). Most modern computers can switch cable type automatically, but to be safe you should use a cross-over Ethernet cable.

You can browse files on the scanner using Windows Explorer using either the serial number or the IP Address 10.0.0.1 (wireless) or 192.168.0.234 (wired) as the network address. Note that DriveVZ400 defaults to using the scanner's serial number… if it cannot connect and you know that you have connected, try opening the IP address in

Windows Explorer first. Sometimes the serial number does not register right away. If your scanner has a different serial number, you must edit the code.

For more detail on connecting to the scanner, check the scanner owner's manual.

Using the program

You only need to be connected to the scanner to use [Fetch] and [Begin Scan]. Otherwise you do not have to maintain a connection to the scanner while the program is running. Note that the conversation with the scanner is stored in "C:\Temp\logfile.txt" for debugging purposes and can be opened after scan completion with [Open Logfile]. At any time you can pop-out the Info Log by double-clicking its title bar. Return it by double-clicking again.

The interface is organized in a logical flow: project setup, site conditions, scan settings, and options. Only the scan settings need change between scans for most sites.

Project setup

Project name

All projects are stored on the scanner or a USB drive plugged into it. Type in a new project name in the entry box, or download a list of existing projects from the scanner and select one. Some notes:

- All projects have a ".riproject" extension. The program will not recognize projects without that extension.
- Existing projects will have a tag appended to their name indicating where the project was detected. These tags are not part of the project name.
    - "(internal)" indicates that the project was found on the scanner's internal drive.
    - "(usb)" indicates that the project was found on the USB drive.
- The Debug option is meant for offline troubleshooting purposes and should not be used in normal operation.

Storage Media

Select where you want the project and scan data to be stored. "USB/Internal" is recommended for nearly all projects—it attempts to save on the USB but will save on the internal drive if no USB drive is detected.

Measurement Program

"High Speed" works for most applications. Using "Long Range" increases scan time by approximately 2.5 times, but can increase measurement range.

Atmospheric conditions

If you brought a thermometer and barometer with you, enter in the atmospheric conditions and the scanner will automatically correct measured values. Temperature is in degrees Celsius, barometric pressure is in millibars, and relative humidity is in %.

Relative humidity has a minimal effect (±0.25ppm if you default to 50%), so do not worry too much about it if you are unable to measure that.

Scan settings

This is the meat of the program. All angles are measured in degrees and define the scan window to be recorded by the scanner. Vertical angles are measured from the vertical axis going down and horizontal angles are measured counter-clockwise from the scanner's power port, up to 720°. See the next section for details on increment precision. Usually you need to do no finer than thousandths of a degree. While running a scan, verify that the parameters received by the scanner are the same as the ones entered.

Common presets are provided based on scan time—add more by editing the VZConfig.cpp code file. The "(Default)" scan does a scan at the coarsest possible resolution. 2min and 5min are good for medium- and high- density 360° scans.

To get an estimate of how long a scan with the given parameters should take, click [Calc Duration]. Note that actual scan time varies from this value.

Scan options

Image Capture

The scanner has a calibrated camera mounted on top of it for collecting images aligned with the scan just taken. Enable this option to have the camera collect a full set of images. The number of images taken depends on the CAM_OVERLAP property, which for now must be set using Telnet or RiSCAN PRO.

There is an option to capture image sets for HDR processing. This feature is still under development. Use at your own risk.

Real-Time Mode

This feature will enable additional features that are needed for real-time analysis. Specifically, the scanner will record highly-accurate inclination values prior to scanning, a low-resolution "monitor file" of the scan will be downloaded to the same directory as the executable, and a text file "vz_info.txt" will be output in the same directory as the executable (by default) that can be parsed by a real-time analysis program (see below).

Go!

Click [Begin Scan] to send all of the settings to the scanner. Verify that the settings were sent correctly by monitoring the text output in the Info log.

Once the scanner has begun scanning, you are free to change the settings in preparation for the next scan. Each new scan in a project opens a new scanposition. The scan can be aborted at any time by clicking [Abort] next to the progress bar.

Scan retrieval

The scanner produces several files with each scan, all of them being time-stamped with the date and time (in GMT) of the scan as its name. The files are stored in a *.riproject folder with the project's name in front, and in the corresponding ScanPos### folder for the current scan position. Note that the RIPROJECT folder will

be either stored on the scanner's internal hard drive or on the USB drive plugged into it, depending on your settings.

These are the files usually stored in the ScanPos### folder upon scan completion:

- YYMMDD_HHMMSS.rxp – the binary raw scan data itself, with housekeeping and monitor data included.
- YYMMDD_HHMMSS.mon.rxp – a small sample of the raw scan data. Useful for real-time change analysis and verifying that the correct area was scanned.
- YYMMDD_HHMMSS.png – a small image file that displays the scan in a polar grid. Useful for easy visual inspection of the scan without having to load the raw data.
- YYMMDD_HHMMSS.pat – an ASCII file with the scan parameters.
- YYMMDD_HHMMSS.prv – a "preview file" that I believe only RiSCAN can use.
- YYMMDD_HHMMSS_Image###.jpg – scan photos taken along the horizontal range of the scan. Some parameters can be read by an ASCII text reader.

Command-line operation

The DriveVZ400 program can be run from the command line for automated operation, with or without user input. This is accomplished by a series of arguments separated by spaces following the executable in a form similar to the following:

```
C:\programs\DriveVZ400.exe m=1 n=20110222_test a=17,1080,41
p=42.134,43.570,.02,321.897,456.123,.02 i=0 r=1
```

The arguments follow a specific format. It is important to note that there must be no spaces within a particular argument for the program to recognize it. The actual order of the tags does not matter, with the exception that the run mode (m,M) must always come first. Here is a rundown of each tag:

- m,M: run mode. This tag must come first!
  - 0—Simply launch the program and ignore all other arguments.
  - 1—Load the arguments into the program and wait for the user.
  - 2 (still to be implemented)—Load the arguments and start the scanner automatically.
- n,N: project name. This is the project name where all of the raw scan data will be stored, usually on a USB drive plugged into the scanner. Remember: there can be NO SPACES, even in folder or project names.
- a,A: atmospheric conditions. This is the air temperature (°C), atmospheric pressure (millibars), and relative humidity (%) of the current environment, separated by commas.
  - Temp range: -50 to 100°C, 1° precision (12° default)
  - Pres range: 600 to 1200mbar, 1mbar precision (1000mbar default)
  - RH range: 0 to 100%, 1% precision (60% default)

- p,P: scan preset pattern. These are preset patterns with all of the parameters set up for you. You'll probably default to the 2min for now. This should be somewhat case-insensitive.
    - "2min"—360° overview at 0.05° increments
    - "5min"—360° overview at 0.03° increments
    - "default"—extremely fast 360° overview... good for testing code
- p,P: (alternate) scan pattern. This is the scan window parameters that set up the actual scan range, separated by commas: vstart,vstop,vincr,hstart,hstop,hincr.
    - vstart: vertical start position. 30 to 130°, 0.001° precision
    - vstop: vertical stop position. same.
    - vincr: vertical angle increment. 0.001 to 0.098750°, 0.000001° precision theoretically (0.0001 practical)
    - hstart: horizontal start position. 0 to 360°, 0.001° precision
    - hstop: horizontal stop position. 0 to 720°, 0.001° precision
    - hincr: horizontal increment. 0.001 to 0.499°, same precision as vertical.
- i,I: images requested. true/false toggle of whether or not images should be recorded.
    - 0—do not record images after the scan
    - 1—if possible, record images after the scan
    - 2 (under development)—do HDR photography
- r,R: operate in real-time mode. You will always have this marked 1.
    - 0—operate normally, recording data as usual.
    - 1—record roll/pitch values prior to the scan, download the monitor file, and write an output file to the executable's directory

Real-time mode

If the user elects to run in real-time mode, an ASCII file named “vz_info.txt” will be created in the same directory as the executable. This file can be parsed by another program upon scan completion to retrieve information needed for real-time analysis. The tags and information in the following line will always remain the same. There will always be a blank line after each tag set.

- #VZ_PROJ: the following line will be a string with the project’s name on the scanner’s storage device.
- #VZ_PATH: the following line will be a string with the path to the downloaded monitor RXP file.
- #VZ_INCL: the following two lines will be floats with the roll and pitch values for the current instrument setup.

Calling another program using Qt

There's a couple ways to run one program from within another. QDesktopServices::openURL() is a very useful function that opens standard files like *.txt or *.doc files using the default program registered with the operating system, but it doesn’t really work for the DriveVZ400 program since there’s no file type associated with it.

QProcess is a class in Qt intended for running programs in another thread. Here's some sample code that calls the DriveVZ400 program using the arguments described above:

```
QProcess* vz = new QProcess(this);
QStringList args;
args    << "m=1"
        << "n=20110222_test23"
        << "a=19,1043,70"
        << "p=35,45,.05,155,165,.1"
        << "i=1"
        << "r=1";
vz->start("C:/programs/DriveVZ400.exe", args);
if(vz->waitForStarted(-1))
        this->userUpdate("Program started!");
qApp->processEvents();  //execute any events collected in the mainEvent queue
                         (such as displaying the line I just output) before
                         executing the child program
if(vz->waitForFinished(-1))
{
        this->userUpdate("Program finished!");
        this->userUpdate(QString("%1").arg(vz->exitCode()));
}
delete vz;
```

`QProcess::start()` runs the child program in a separate thread, so the host/parent program will still be running at the same time under another process. The `QProcess::waitForStarted(-1)` and `QProcess::waitForFinished(-1)` functions lock the parent program until an exit signal is received from the child program. These functions are not required, but they can be helpful if your parent program cannot continue without the scan information.

APPENDIX D – RESULTS OF A SURVEY OF TLS PROFESSIONALS

Industry survey of TLS Professionals

This is a detailed summary of a survey conducted in September through lidarnews.com (13 responses) and in October through laserforums.uk (35 responses). Text-based responses are time-stamped in order to provide cross-referencing.

Question 1

What is the make and model of your laser scanner(s)?

Count:	48
Leica HDS Scan Station 2	9/28/10 12:53AM
Leica C10 Leica 6100	9/26/10 5:32PM
Trimble GS 101	9/24/10 9:14PM
FARO	9/24/10 7:32PM
HDS 6000 ScanStation LS880	9/24/10 4:07AM
HDS3000	9/24/10 3:17AM
faro ls 120	9/24/10 1:47AM
Riegl 390i	9/24/10 1:25AM
ScanStation C10	9/23/10 6:29PM
I have worked exclusively with Trimble scanners - mainly the GXA	9/23/10 3:17AM
Leica ScanStation	9/22/10 8:59PM
Trimble FX	9/22/10 8:08PM
FARO - Photon 120	9/22/10 7:24PM
Leica C10	9/22/10 7:02PM
Leica SSII	9/22/10 6:14PM
Leica c10	9/22/10 5:59PM
Faro Photon 120 Leica Scan Station 2	9/22/10 4:21PM
ILRIS-3D	9/22/10 10:33AM
Riegl LMS Z620, Leica C10, Leica HDS6100	9/22/10 7:54AM
Leica C10	9/22/10 5:35AM
Leica HDS 3000	9/22/10 4:52AM
Topcon GLS-1500	9/22/10 4:43AM
Riegl VZ400 Leica 3000	9/22/10 4:39AM
Leica C10	9/22/10 4:30AM
Leica C10 laser scanner	9/22/10 2:42AM
Leica 3000 and Cyrax 2500	9/22/10 12:54AM
Leica C10	9/22/10 12:19AM
Leica Scanstation HDS 3600	9/21/10 11:59PM
Leica Scan Station C10	9/21/10 11:54PM
HDS2500	9/21/10 10:52PM
FARO LS880	9/21/10 10:26PM
Leica HDS3000	9/21/10 7:55PM
Leica SS2	9/21/10 6:06PM
Leica C10 HDS6100	9/21/10 5:52PM
Optech ILRIS 36D	9/21/10 5:31PM
Leica C10 Scanstation	9/21/10 5:09PM
All Leica, HDS3000, ScanStation ScanStation 2, C10 and HDS6*00	9/21/10 4:26PM
Leica C10	9/21/10 1:24PM
leica scanstation 2	9/18/10 4:01AM
Leica C-10	9/11/10 4:28AM
Leica Scanstation	9/7/10 2:08AM

Riegl Z420i	9/6/10 1:21PM
Leica Scanstation 2	9/4/10 6:11AM
Leica ScanStation2 Leica ScanStation C10	9/4/10 4:25AM
Z+F	9/3/10 11:44PM
Leica Scanstation2, C10 , Surphaser and Riegl	9/3/10 10:48PM
Leica ScanStation C10	9/3/10 2:35PM
Leica Scansation C10 and Scanstation 2	9/3/10 3:15AM

Question 2

Does your scanner have a level compensator?

Count:	48
Yes	39
No	8
Not sure	1
What are level compensators?	0

Question 3

If yes, how often do you use your level compensator when scanning? (response not required)

Count:	40
I'm not sure	0
Every time	22
Most of the time	11
Occasionally	3
Rarely	2
Never	2

Note
1 respondent said he used his compensator every time, but he entered in the previous question that he doesn't have one. I altered the Every Time category from 23 to 22 to reflect that discrepancy.

Question 4

Why do you use or not use a level compensator? (response not required)

Count:	37
Stopped using it because it slows down the scan speed and takes to long to establish control for the scan setups. Didn't notice any difference in accuracy.	9/28/10 12:53AM
We always scan level, with no need for inverted scanners etc. Why wouldn't you use a compensator? Relying on targets alone seems a step backwards. The standard deviations in height for targets after registration gives you a good QA check on level consistency in your scan cloud.	9/26/10 5:32PM
It does not have any negative effect but supports registration a lot.	9/24/10 7:32PM
We use it during scanning but don't always use it for registration, depends on the residuals.	9/24/10 4:07AM
We use it because it is available	9/24/10 1:47AM
Orientation is better defined through a control network	9/24/10 1:25AM

Because I want levelled data pretty much 100% of the time as the work is survey-grade. I wouldn't turn off a DAC on a TPS...	9/23/10 6:29PM
The introduction of the dual axis compensator was a tremendous advancement in the emerging hardware platforms. The compensator allows the individual to setup and level up over a known point and observe a single control point. This is a far superior solution o "photogrametric" scanning solutions that require three or more control points. The residuals for the control network are displayed immeadiately, confirming that the cloud registration is within expected tolerances. The dynamic compensator provides corrections during the data capture process, which can be introduced by wind and or vibration. The quality of the data with the compensator on verses off can be substantional.	9/23/10 3:17AM
Always use, might not use when I take images some times but always when scanning.	9/22/10 8:59PM
Use it to improve quality of the scans and be able to correct problems if they appear.	9/22/10 7:02PM
generally level all targets usig a total station anyway, so sometimes dont use level compensator to speed up the process..	9/22/10 6:14PM
Allows easier cloud to cloud (2 picks). Also i'm a true surveyor and we like eveything to be levelled.	9/22/10 5:59PM
We have switched the compensator off on the scanstation to increase speed and in environments where the scanner needs to not be levelled (scanning a ships deck) However with the Faro we leave it on nearly all the time.	9/22/10 4:21PM
Depends on control methodology as to whether I use a the compensators. Whenever I set up directly over a mark the compensators are engaged. Where suitable I will always utilise the compensators	9/22/10 7:54AM
Saves setting up extra targets	9/22/10 5:35AM
I use it to ensure that I am getting the best data that I can, the only time I have turned it off is when there is a lot of foot trafic around the tripod while indoors.	9/22/10 4:43AM
It is a nice backup and makes bad control easier to find. Some situations limit control.	9/22/10 4:39AM
Using it seems to keep a real tight registration with targets.	9/22/10 2:42AM
Having the ability to level a scan means a higher degree of accuracy can be maintained and control for each scan.	9/22/10 12:19AM
If we are scanning an area that has vibration of from large truck or trains. This vibration keeps making scanner switch to the next scan world. We will disable the Level compensator and up sphere targets to help tie the scans together.	9/21/10 11:59PM
I use one because a) it means I can be confident in any individual scan being level, and b) I can use it as control which allows me to only use two targets in addition to this in each scan.	9/21/10 11:54PM
It doesnt have a level compensator.	9/21/10 10:52PM

The compensator is used in most applications with the primary exception being high accuracy scanning in which a large number of control targets are used and the z axis of the scanner is not able to be plummed.	9/21/10 10:26PM
Do not use it when the setup might not be steady enough and has vibrations (ship deck, vibrating plant) when compensator might give erroneous readings.	9/21/10 5:52PM
LC lowers accuracy. dual mirror system provides a very precise measurement routine in a internally fixed coordinate system - once the scans are aligned to each another and geo-referenced, values from the lc are redundant. I guess lc's are needed for close range indoor scanning but not for long range out door activities (as you will need several setups with precise gps coordinates for each scan origin...	9/21/10 5:31PM
We'll turn it off if the scanner has to be used while non-level. Boats, ships. While tilted to achieve more down angle.	9/21/10 5:09PM
not use when on a boat or a moving object, when the scanner is moving at the same rate as the object. Use all the time the SS2 and C10 are survey instruments.	9/21/10 4:26PM
The compensator gives you a virtual target many kms up in the air.	9/21/10 1:24PM
On a project where we used it, we had a great deal of difficulty getting good results with the registration. Using 4 targets and the resection method gives us much better results	9/18/10 4:01AM
Allows individual scans to be controlled using fewer unknowns during registration	9/11/10 4:28AM
To obtain at least one scan with real verticality of the site.	9/7/10 2:08AM
Aids in the accuracy when using a single target backsight method	9/6/10 1:21PM
We use our laser scanner mostly for topographic surveys. Under changing weather conditions or unstable surfaces (e.g. hot asphalt), the weight and movement of the scanner can quickly cause the instrument to become out-of-level. As the target-based control is acquired by the scanner at the beginning of the scan session, the compensators' adjustments ensure a reasonable amount of accuracy throughout entire scanning process.	9/4/10 6:11AM
With the compensator on we can traverse with the scanners and only need 2 tragets, at the backsight and foresight.	9/4/10 4:25AM
Tppography/infrastructure/long range <100m, yes, other apps- seldem. .	9/3/10 10:48PM
a) Setup methods like known backsight or traversing require a levelled instrument. b) Scans of longer duration: Compensator compensates slight movements due to sunlight or other effects.	9/3/10 2:35PM
Using the scan station 2, i would not use the compenstor in awkward situations where a using a tripod is not possible or practical, however occasionally it may be used for a time saving reasons where there is only a limited window. Whereas because the c10 can be levelled using the tri-brach it will always be used levelled, as the speed of it usually negates the need to turn it off.	9/3/10 3:15AM

Question 5

Do you use target-based registration or some other technique to georeference and combine scans? (multiple selections allowed)

Count:	104
I'm not sure	0
Target-based registration	46
Software-based point cloud surface matching (e.g. Iterative Closest Point - ICP)	24
Manually pick common points from point cloud	21
Other (please specify)	13

Others

We also use the amberg GRP5000FX systems for mobile scanning in rail environments. Registration in this sense is a chainage based process.	9/26/10 5:32PM
Combination of all above - job dependent	9/23/10 6:29PM
on-the-fly target registration for immeadiate registration reports and control confidence	9/23/10 3:17AM
Traverse and backsighting from known point to known point	9/22/10 8:59PM
Using the inclinator gives us a backup if some targets are missed.	9/22/10 4:21PM
We use occupy and back site as well as target registration, which ever is better for the situation.	9/22/10 4:43AM
External survey control generated by a total station.	9/21/10 11:54PM
GPS coordinates for scan origin (mostly used technique)	9/21/10 5:31PM
Cloud to Cloud	9/21/10 4:26PM
A mixt of techniques depending on the results to be obtained.	9/7/10 2:08AM
I'm a big fan of target based resections through known control. Although requires preparation, it combines mobility benefits of cloud surface matching with the some of targeted based registration.	9/4/10 6:11AM
modeled objects	9/3/10 10:48PM
very rarely i have modelled surfaces or objects to use as registration items.	9/3/10 3:15AM

Question 6

When registering your scans, do you constrain the scan alignment to use the values from the level compensators? (select the most appropriate option)

Count:	48
Yes	24
No	5
I don't use a level compensator	8
It depends (please explain)	11

Others

Not sure what you mean. Dont think I knew about that.	9/28/10 12:53AM
Not when using the Leica 6100, as we are only relying on the bubble. When scanning on our extendable tripod up to 3 metres in height we may not use the compensator if confident the setup is stable. in this case we rely on targets, as it is often difficult to physically level the scan head to within compensator tolerance.	9/26/10 5:32PM

If the residuals are better with the compensator turned off, then we visually inspect the scan for double clouding and if there is none then we leave the compensator off.	9/24/10 4:07AM
some times the compensator does not work well when stiching the scans together. In that case we will disable it.	9/24/10 1:47AM
I use Faro's inclinometer ON setting to register our scans.	9/22/10 7:24PM
Only if control is not available in quantity or quality	9/22/10 4:39AM
Not during high accuracy scanning in which a large number of control targets are used and the z axis of the scanner is not able to be plummed.	9/21/10 10:26PM
Depands on the solution of registration and site conditions	9/21/10 5:52PM
The Leica compensator is either on, or off. If off then we switch to a more complete cloud to cloud or multitarget system. If it's on, then we treat the clouds as levelled. The compensator used is the same as in the Leica total stations.	9/21/10 5:09PM
yes when using a scanner with a DAC, and never if it doesn't even when the software wants to think that slightly out of level is good enough.	9/21/10 4:26PM
Very rarely	9/3/10 10:48PM

Question 7

What software package(s) do you use for scan alignment?

Count:	48
Cyclone	9/28/10 12:53AM
cyclone latest version. Amberg TMS.	9/26/10 5:32PM
Trimble Realworks	9/24/10 9:14PM
SCENE	9/24/10 7:32PM
Cyclone	9/24/10 4:07AM
Cyclone v6	9/24/10 3:17AM
Faro Scene	9/24/10 1:47AM
Riscan/Cyclone	9/24/10 1:25AM
Cyclone Register	9/23/10 6:29PM
The alignment is performed in the field - Trimble Pointscape or Trimble Access	9/23/10 3:17AM
Leica Cyclone	9/22/10 8:59PM
Trimble Realworks	9/22/10 8:08PM
FARO Scene 4.7	9/22/10 7:24PM
Leica Cyclone	9/22/10 7:02PM
Cyclone	9/22/10 6:14PM
Cyclone, pointools, geomagic	9/22/10 5:59PM
Faro Scene / Cyclone 7.2	9/22/10 4:21PM
Polyworks	9/22/10 10:33AM
Riscan, Cyclone	9/22/10 7:54AM
Cyclone register	9/22/10 5:35AM
Leica Cyclone, Leica Cloudworx, software developed by my company	9/22/10 4:52AM
Topcon's Scan Master Software	9/22/10 4:43AM
RiScan Pro or Cyclone	9/22/10 4:39AM
Leica Cyclone	9/22/10 4:30AM
Leica Cyclone	9/22/10 2:42AM

Cylcone	9/22/10 12:54AM
Leica Cyclone	9/22/10 12:19AM
Cyclone	9/21/10 11:59PM
Cyclone	9/21/10 11:54PM
Leica Cyclone [REGISTER]	9/21/10 10:52PM
FARO Scene	9/21/10 10:26PM
Cyclone	9/21/10 7:55PM
Cyclone	9/21/10 6:06PM
Cyclone	9/21/10 5:52PM
JRC 3D Reconstructor 2; PolyWorks	9/21/10 5:31PM
Cyclone	9/21/10 5:09PM
Cyclone	9/21/10 4:26PM
Leica Cyclone	9/21/10 1:24PM
Leica Cyclone 7.0	9/18/10 4:01AM
Leica, Faro, custom	9/11/10 4:28AM
Cyclone	9/7/10 2:08AM
RiScan	9/6/10 1:21PM
Leica Cyclone 6	9/4/10 6:11AM
Leica Cyclone 7	9/4/10 4:25AM
Propietary of Z+F and LFM	9/3/10 11:44PM
Cyclone, Rapidform	9/3/10 10:48PM
Leica Cyclone Register	9/3/10 2:35PM
Leica Cyclone 7	9/3/10 3:15AM

Question 8

Please share any comments or experiences you might have

Count:	17
When mixing 6100 and C10 data, having the added constraint of a compensator in the C10 data greatly helps with overall scan cloud accuracy. Registering the compensated data first then registering the un-compensated 6100 data to the compensated data also aids in overall consistency with the data. We treat compensated data as a being of a higher order of accuracy.	9/26/10 5:32PM
Inclination sensor information helps in many cases to reduce the ammount of needed targets. Or, in case to few targets are in sight, it helps to register the scans at all.	9/24/10 7:32PM
Will you publish the results on the Laser Scanning Forum?	9/24/10 3:17AM
Never let an untrained person use a scanner - you will never get the results are (or they) are expecting!	9/23/10 6:29PM
The ability to register scans "on-the-fly" provides a superior solution to cloud based regsitration. The registered scans are viewable in the field and quickly identify areas of concern, data gaps or descrepencies.	9/23/10 3:17AM
leica c10 seems to be fine with the compensator on all the time, even in high wind.	9/22/10 5:59PM
Most of the work I do makes the ILRIS the best overall choice, but I still view its lack of a dual-axis compensator as a negative.	9/22/10 10:33AM
Coming from a survey background control and the use a compensators are the critical factors for scanning projects	9/22/10 7:54AM

The Topcon scanner and software is by far one of the most accurate and easy to use time of flight scanners on the market.	9/22/10 4:43AM
Control is the key to any good scan/survey. It is amazing how lack of knowledge and understanding can ruin good intentions.	9/22/10 4:39AM
The HDS3000 requires 4 control points, each in a sector surrounding the scanner for every setup, otherwise the overlapping data between scans shows a separation that becomes very difficult to deal with. The sun is really hot in South Africa so we often experience changes in the tilt of the scanner due to the sun being on one side, and regular target checks often reveal horrendous changes in the elevation of targets at 50 - 100m. We recently used 2 C10's for a highway scanning project (We are still getting into mobile scanning) and never experienced any separation issues even using only 2 control targets at times. We had no sun issues either. Very impressed with the compensator for this type of work, but understand the issues behind the speed of the laser vs the rate of compensation, and that the compensator can hinder the laser acquisition rate.	9/21/10 7:55PM
In case, you did not mean an ordinary inclinometer but a dual axis compensator, this is not included in the ILRIS. Nevertheless, the highest accuracy you can get is by aligning all the scans via ICP and later georeference via GPS coordinates for each origin of the scan's coordinate system. As the ILRIS has a very precise inherent implementation of a measurement coordinate system, a compensator is not needed. Dual axis compensators are needed for one mirror and rotating base systems...	9/21/10 5:31PM
Your original question is flawed, a compensator and inclinometer are not the same thing. you need to be careful how you interpreted the 2 results depending on the scanner in use. I lecture (I am not a teacher) the use of scanning and am appalled all the time to find surveyors do not know what a compensator is or what it can do for them. virtually all registrations I get to see from non compensated (lots) scanners normally have issues and are poorly registered.	9/21/10 4:26PM
feel free to contact with question Joseph Chumbley Lockheed Martin xxx.xxx.xxxx	9/11/10 4:28AM
In large works we always assure the targets with traversing w/total station. This eliminates any risk of non closure.	9/3/10 11:44PM
SS2 with compensator is much slower so we sometime start with comp' and turn it off later	9/3/10 10:48PM
Previously I have not used a compensator when using the SS2 in the roof space of a old building. The roof had very limited clearance, and was unsafe in places, so was placed in locations where it was safe to get to. I have also not used the compensator when mapping cliff faces, to maximise the available tidal window! this was also as sufficient wide ranging control stations and targets could be established at the extremeties of the scan to allow for reliable verticality controls	9/3/10 3:15AM